在脉冲星测时阵列中寻找引力波背景

黄庆国

中国科学技术大学，合肥
中国科学院理论物理研究所

08/Dec/2023

Image courtesy of *Science*, credit: Nicolle Rager Fuller *[modified]*

Newton's law of Gravity

$$F_G = G\frac{m_1 m_2}{r^2}$$

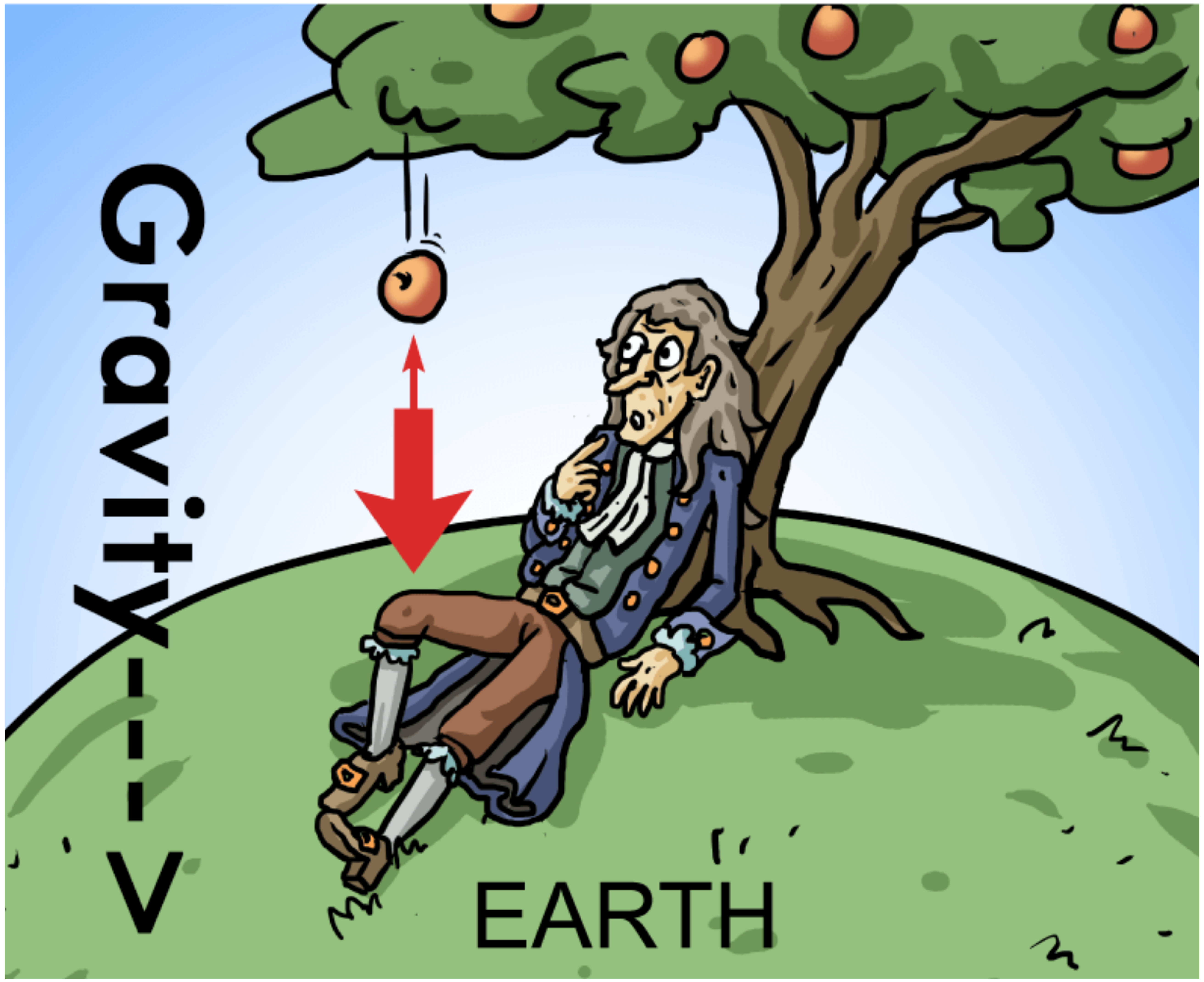

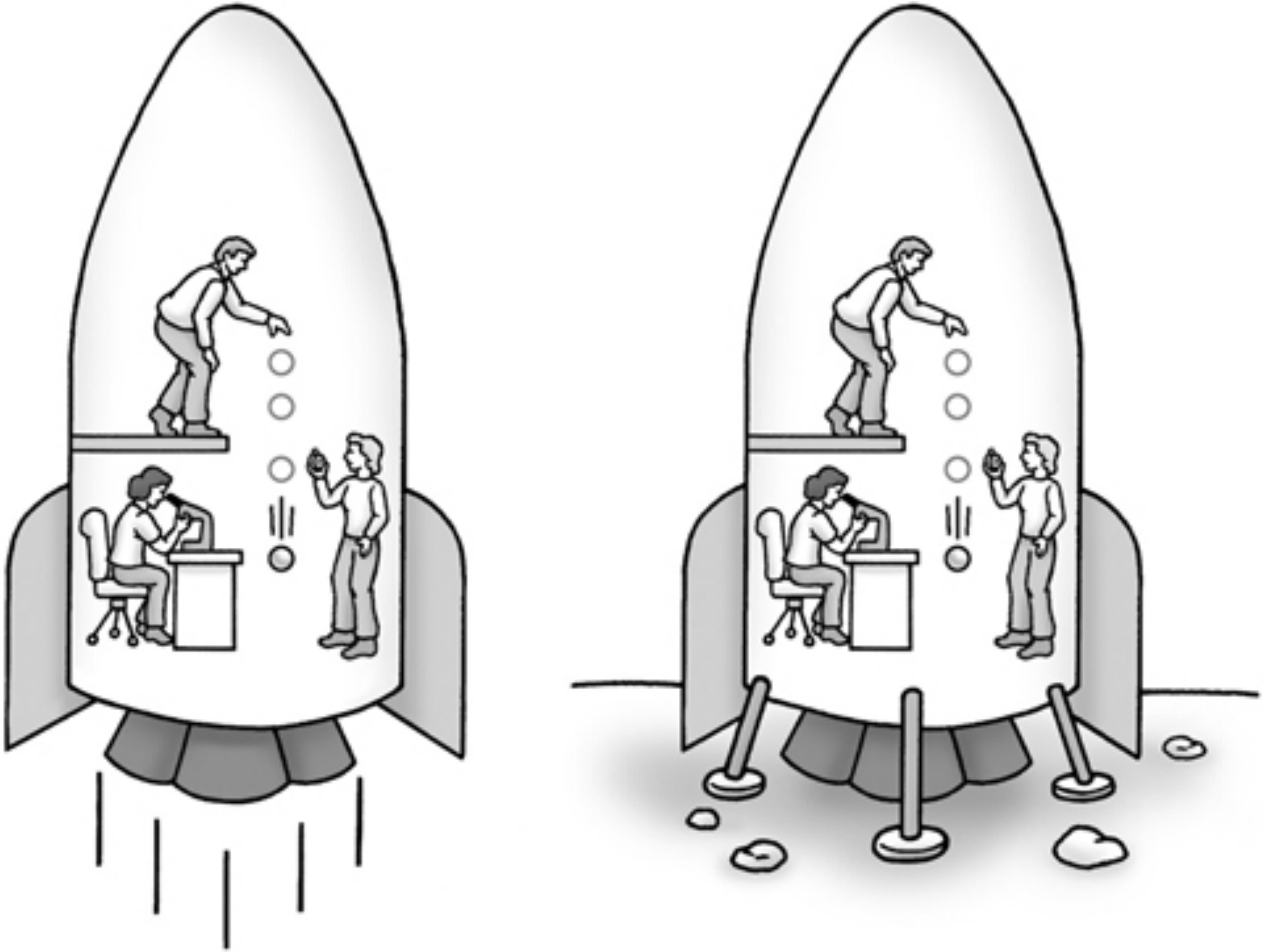

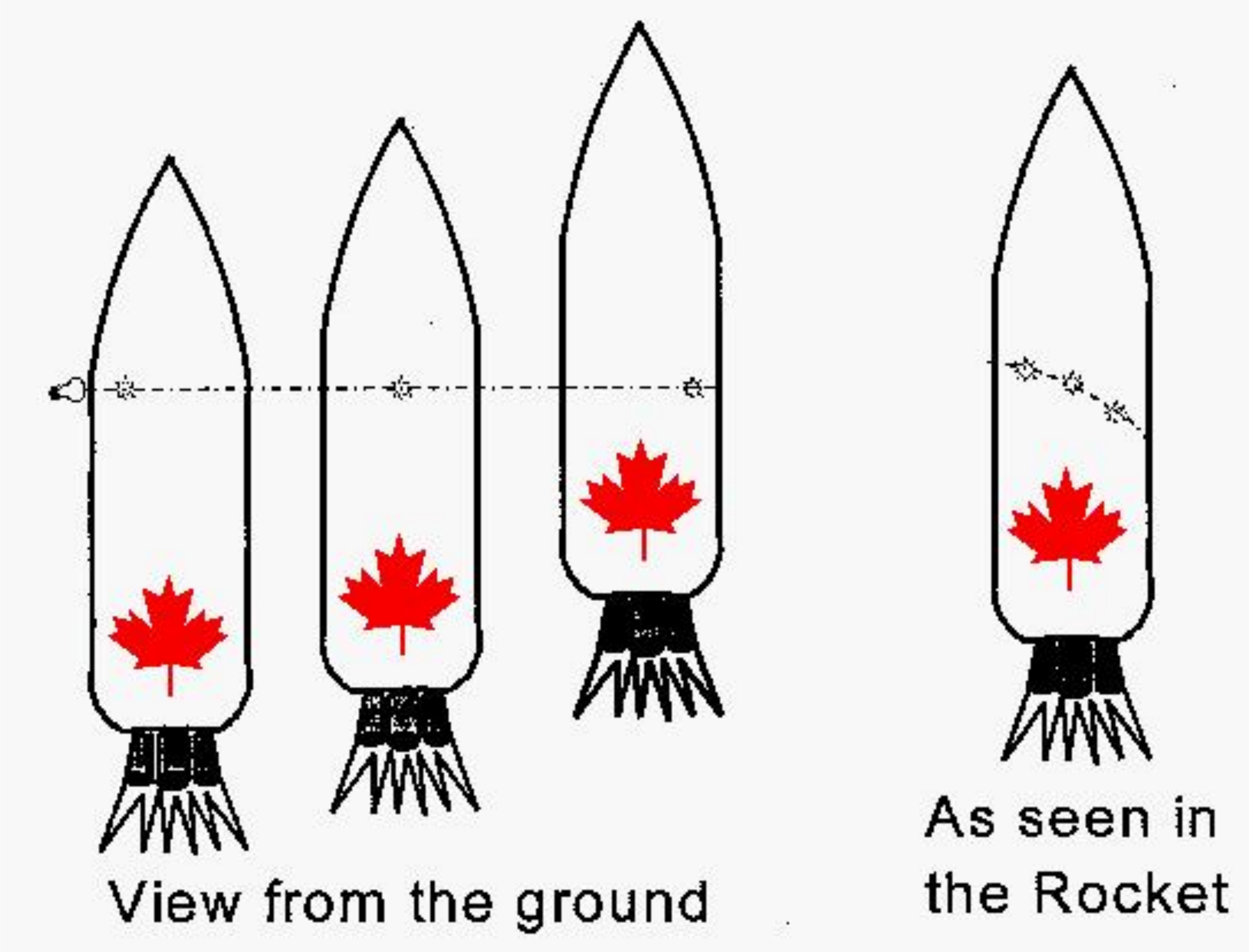
View from the ground
As seen in the Rocket

Einstein’s General Relativity

$$R_{\mu\nu} - \frac{1}{2}Rg_{\mu\nu} = 8\pi G T_{\mu\nu}$$

Gravitational Waves

$$g_{\mu\nu} = \eta_{\mu\nu} + h_{\mu\nu}, \quad \Box h_{\mu\nu} = 0$$

Physics 1993

R. Hulse and J. Taylor

For measurements of the Hulse-Taylor binary system that provides indirect evidence for existence of gravitational waves.

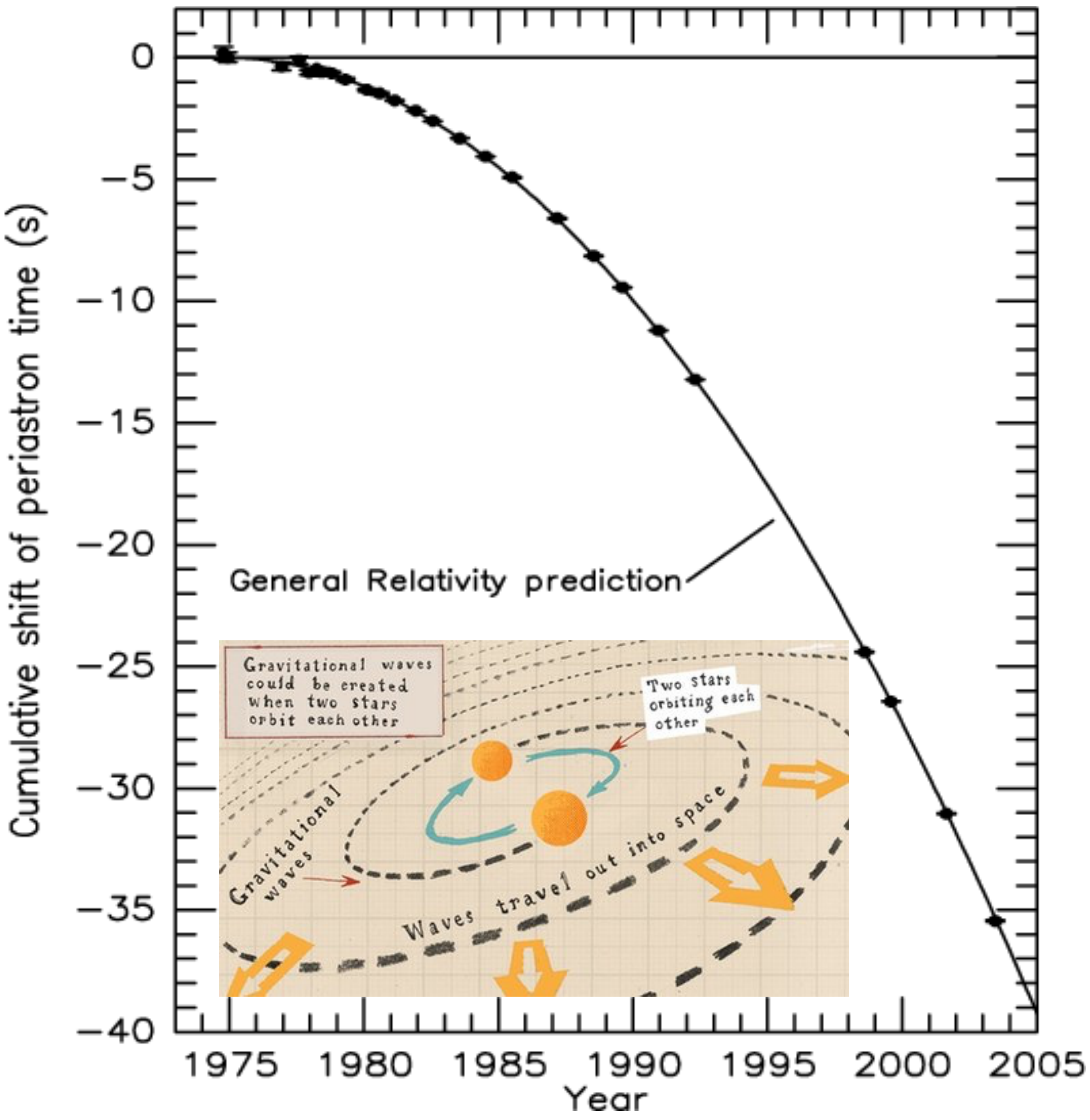

Physics 2017

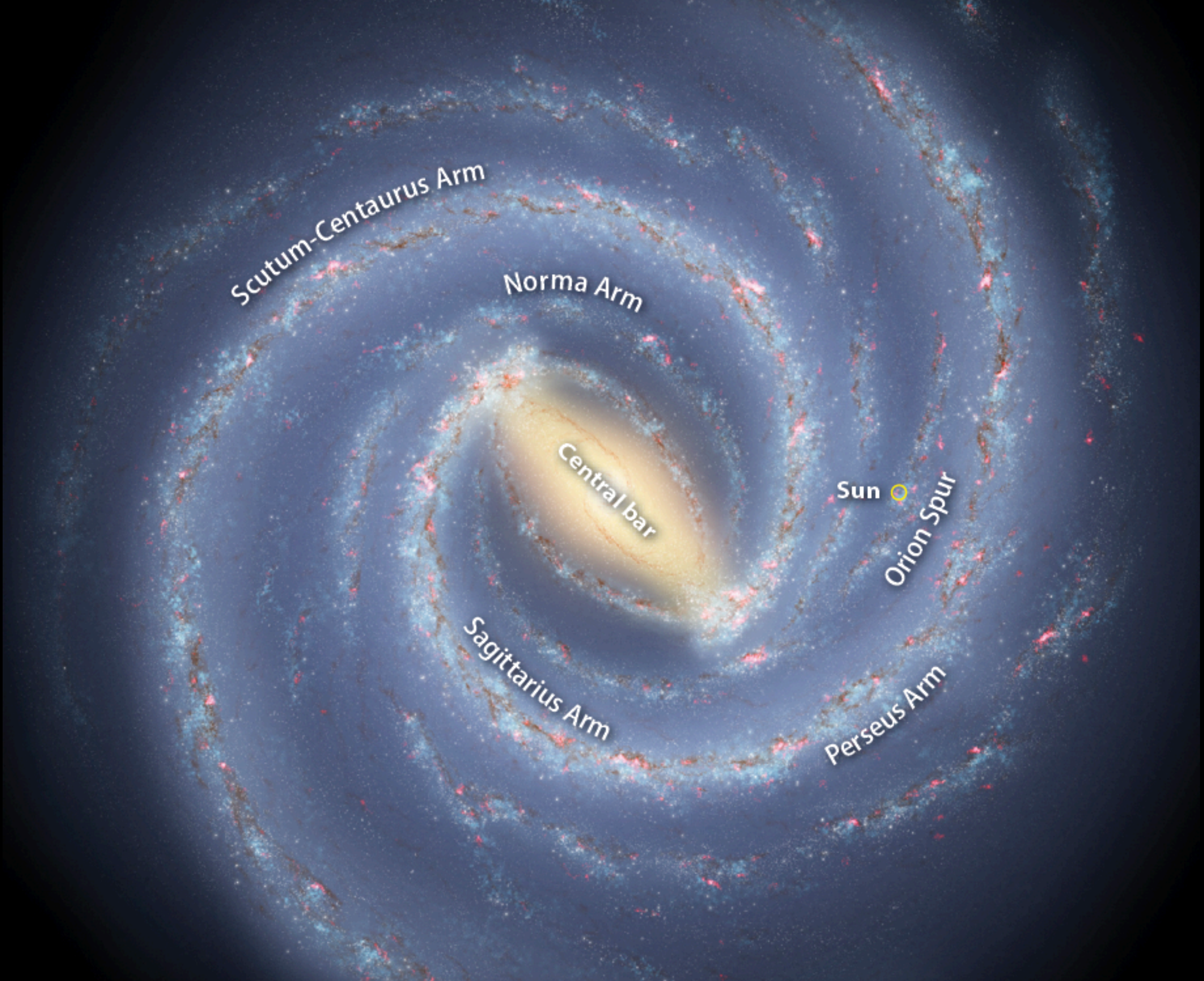

Credit: https://www.astronomy.com/science/how-the-milky-way-got-a-brand-new-look/

Physics 2020

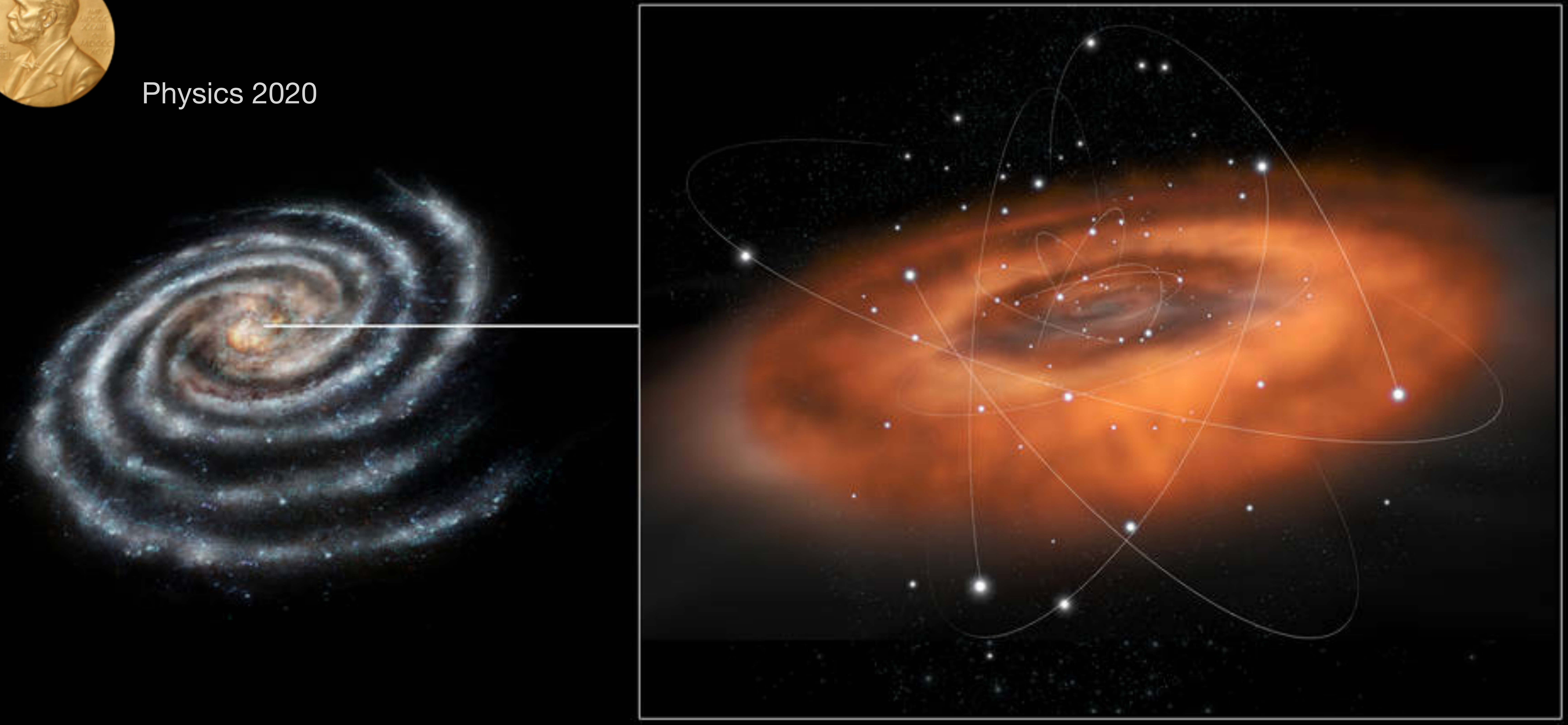

Credit: https://www.nasa.gov/mission_pages/herschel/multimedia/pia17009.html

The gravitational wave background (GWB) is formed by many different overlapping gravitational-wave signals emitted from the cosmic population of supermassive binary black holes and/or other cosmological processes.

Credit: https://stockiner.com/gravitational-wave-background-discovered-entire-universe-is-filled-with-the-buzz-of-extremely-long-wavelength-space-time-oscillations/

The Gravitational Wave Spectrum
Sources
Detectors
Big Bang
Supermassive Black Hole Binary Merger
Compact Binary Inspiral & Merger
Extreme Mass-Ratio Inspirals
Pulsars, Supernovae
Wave Period
age of the universe
years
hours
seconds
milliseconds
10^-16
10^-14
10^-12
10^-10
10^-8
10^-6
10^-4
10^-2
1
10^2
Wave Frequency
CMB Polarization
Radio Pulsar Timing Arrays
Space-based interferometers
Terrestrial interferometers
David Champion

Gravitational-Wave Spectrum and Hellings-Downs Curve

The timing-residual cross-power spectral density

$$S_{ab}(f) = \Gamma_{ab}\frac{A_{GWB}^2}{12\pi^2}\left(\frac{f}{f_{yr}}\right)^{-\gamma} f_{yr}^{-3}$$

where $\gamma = 3 - 2\alpha$ (so the SMBHB $\alpha = -2/3$ corresponds to $\gamma = 13/3$).

The energy spectrum of GWB

$$\Omega_{GW}(f) = \frac{1}{\rho_c}\frac{d\rho_{GW}}{d\ln f} = \frac{2\pi^2 A_{gw}^2}{3H_0^2}\left(\frac{f}{f_{yr}}\right)^{5-\gamma} f_{yr}^2$$

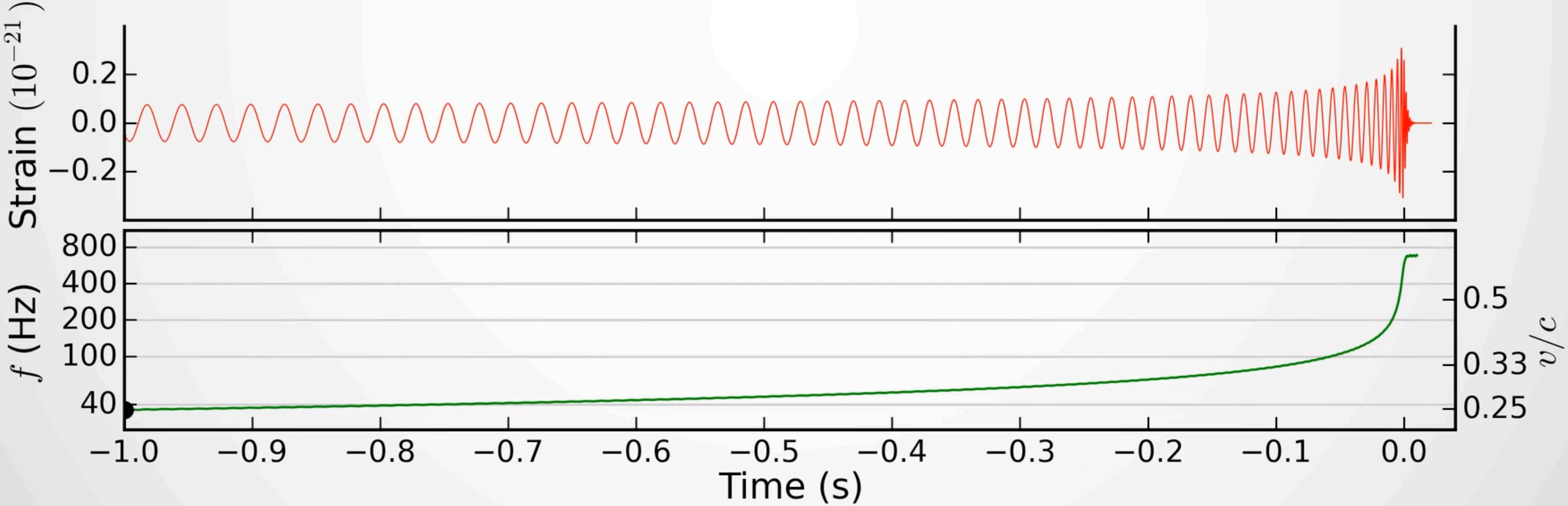

$$\Gamma^{TT}_{ab}(f) = \frac{3}{8\pi}\int d\Omega \left(e^{2\pi i f L_a(1+\mathbf{\Omega}\cdot\mathbf{p}_a)} - 1\right)\left(e^{2\pi i f L_b(1+\mathbf{\Omega}\cdot\mathbf{p}_b)} - 1\right)\sum_{A=+,\times} F^A_a(\mathbf{\Omega})F^A_b(\mathbf{\Omega})$$

$$= \frac{1}{2}(1+\delta_{ab}) + \frac{3}{2}k_{ab}\left(\ln k_{ab} - \frac{1}{6}\right)$$

The antenna pattern: $F^A(\mathbf{\Omega}) = \frac{1}{2}\frac{\mathbf{p}^i\mathbf{p}^j}{1+\mathbf{\Omega}\cdot\mathbf{p}}e^A_{ij}(\mathbf{\Omega})$

$k_{ab} = (1-\cos\xi_{ab})/2$

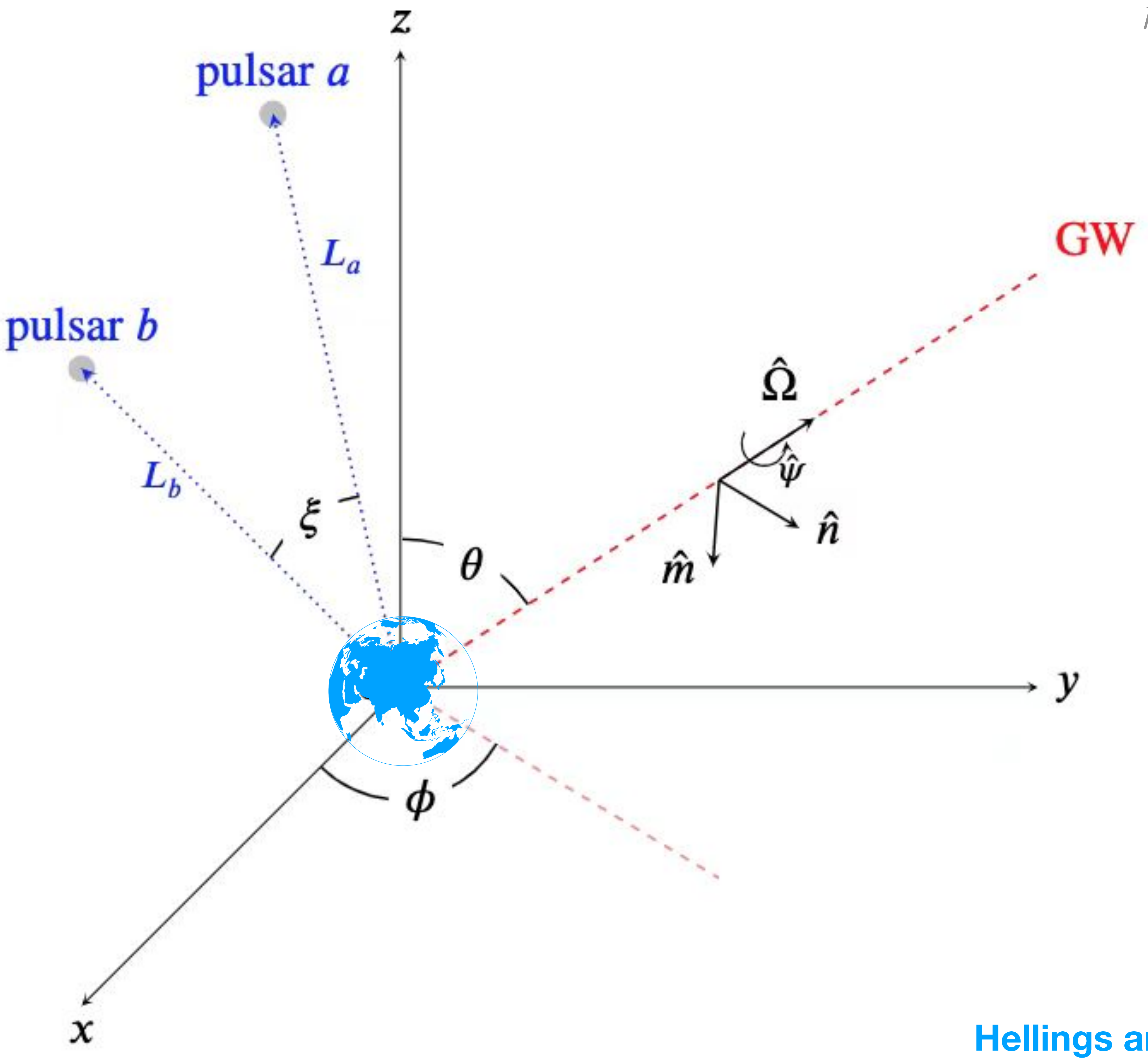

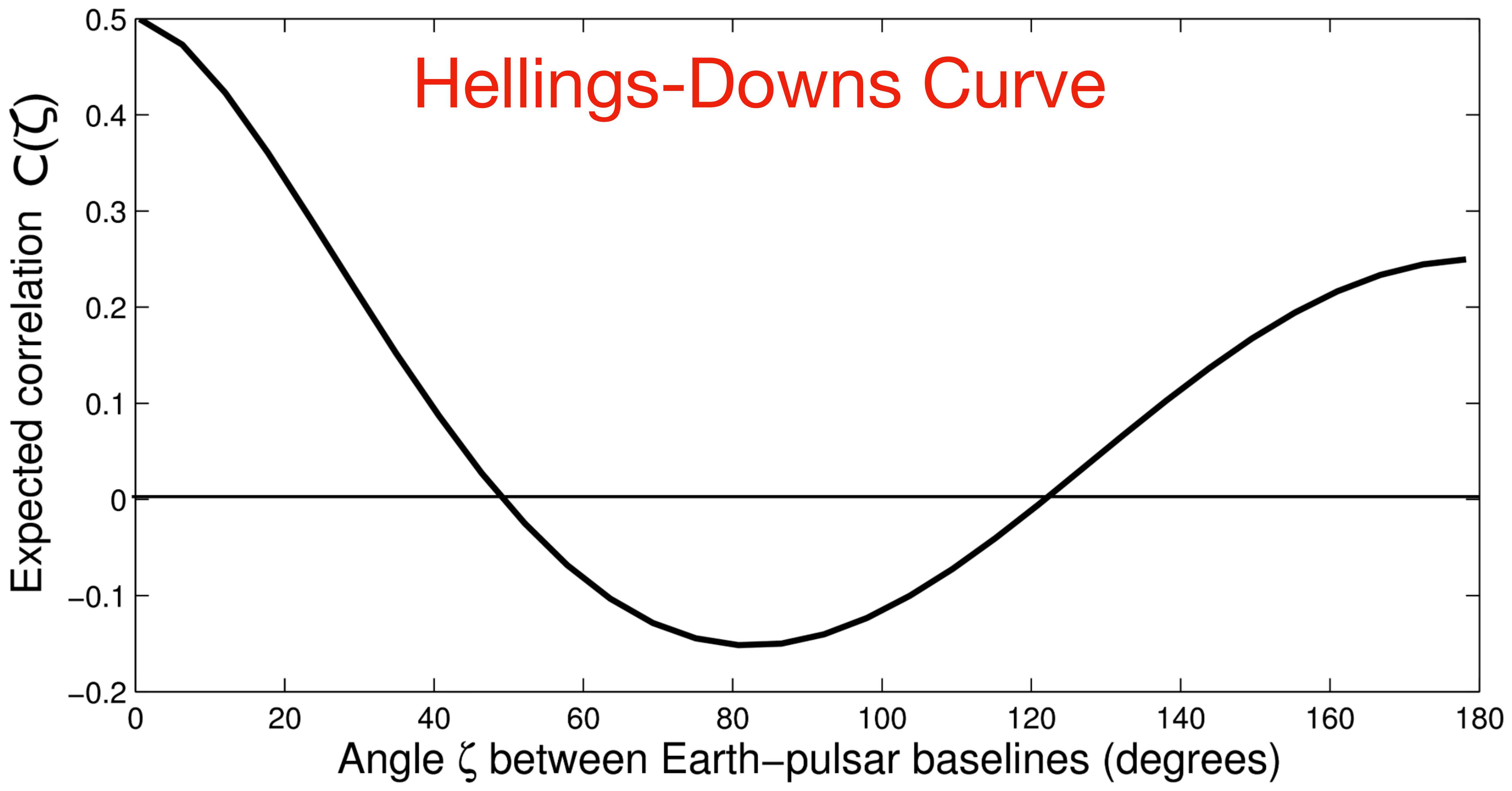

Hellings and Downs, ApJ 265, L39 (1983)

NANOGrav 15-year

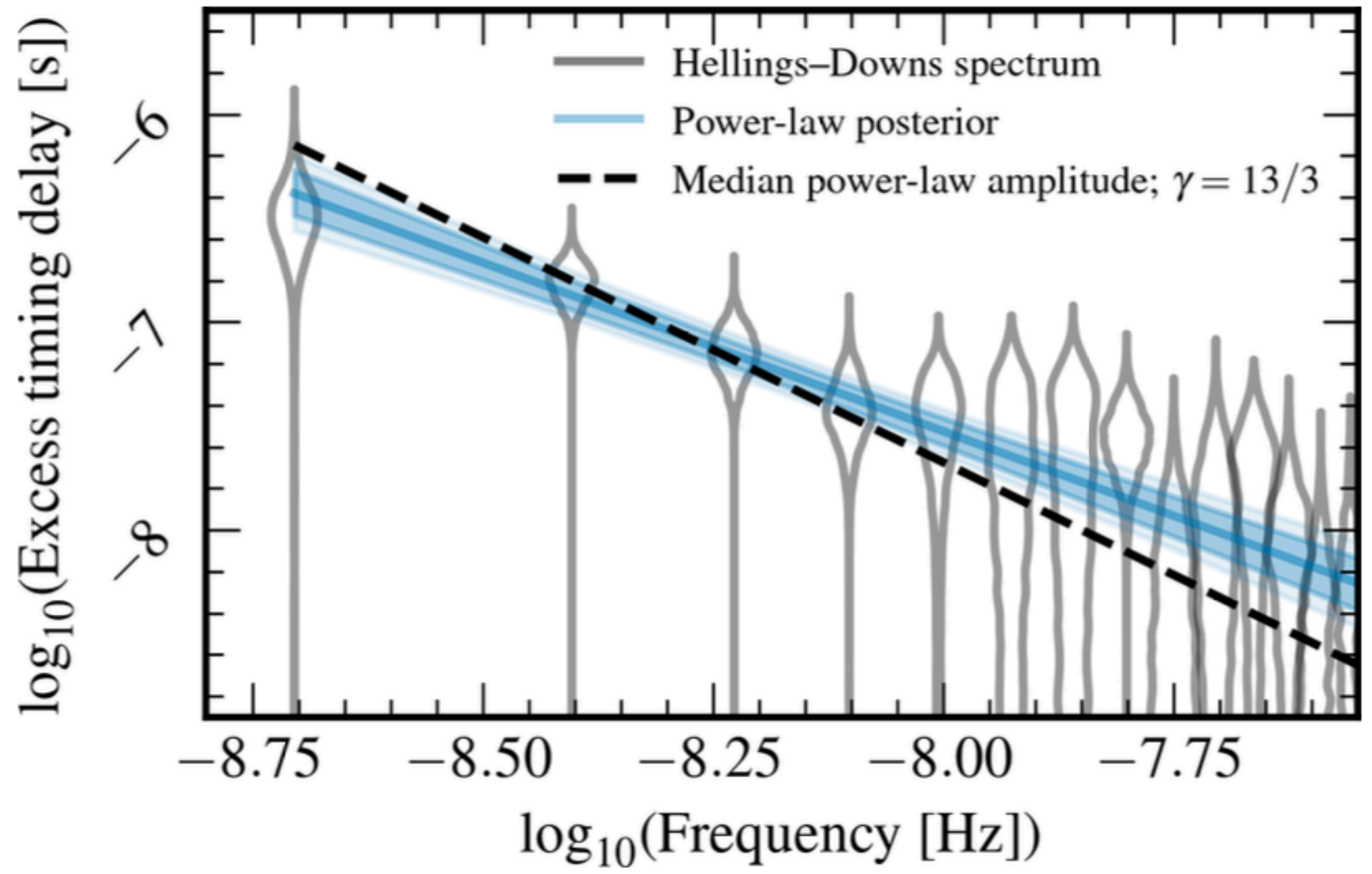

(b)

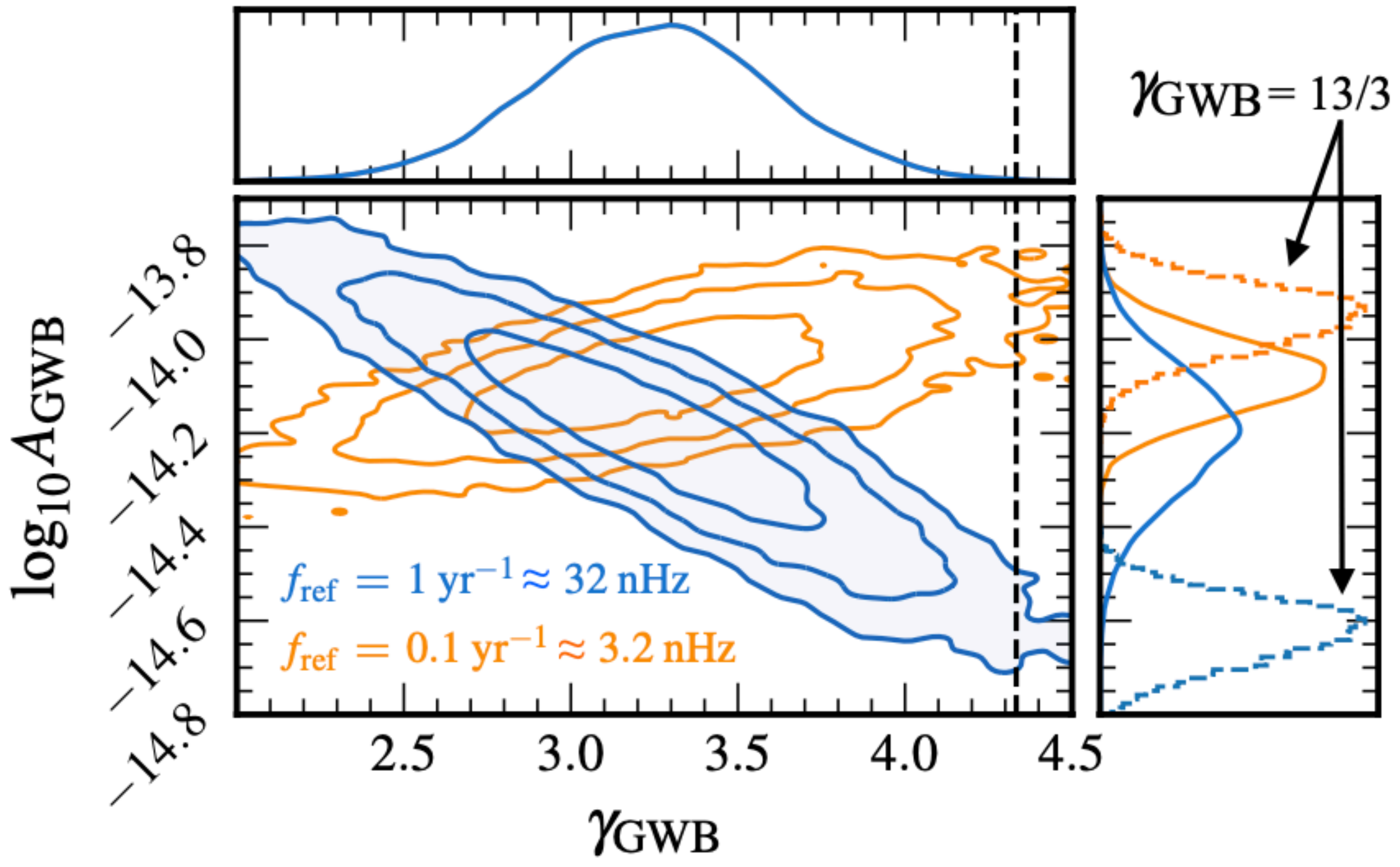

EPTA DR2

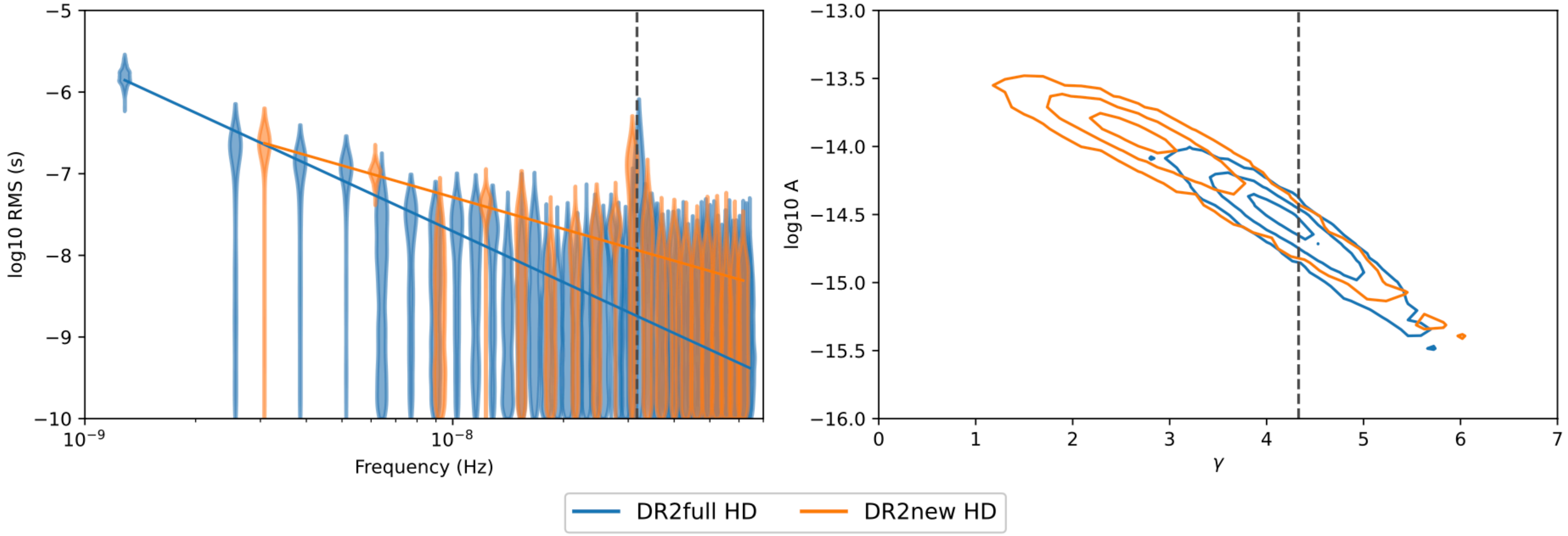

PPTA DR3

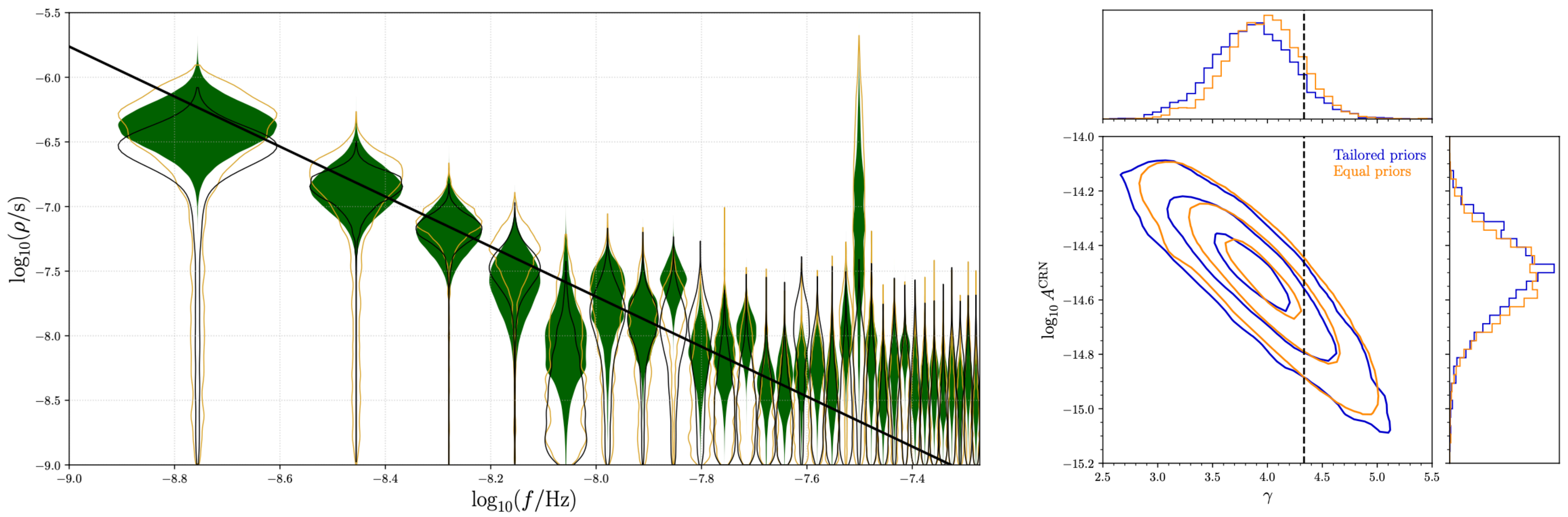

CPTA DR1

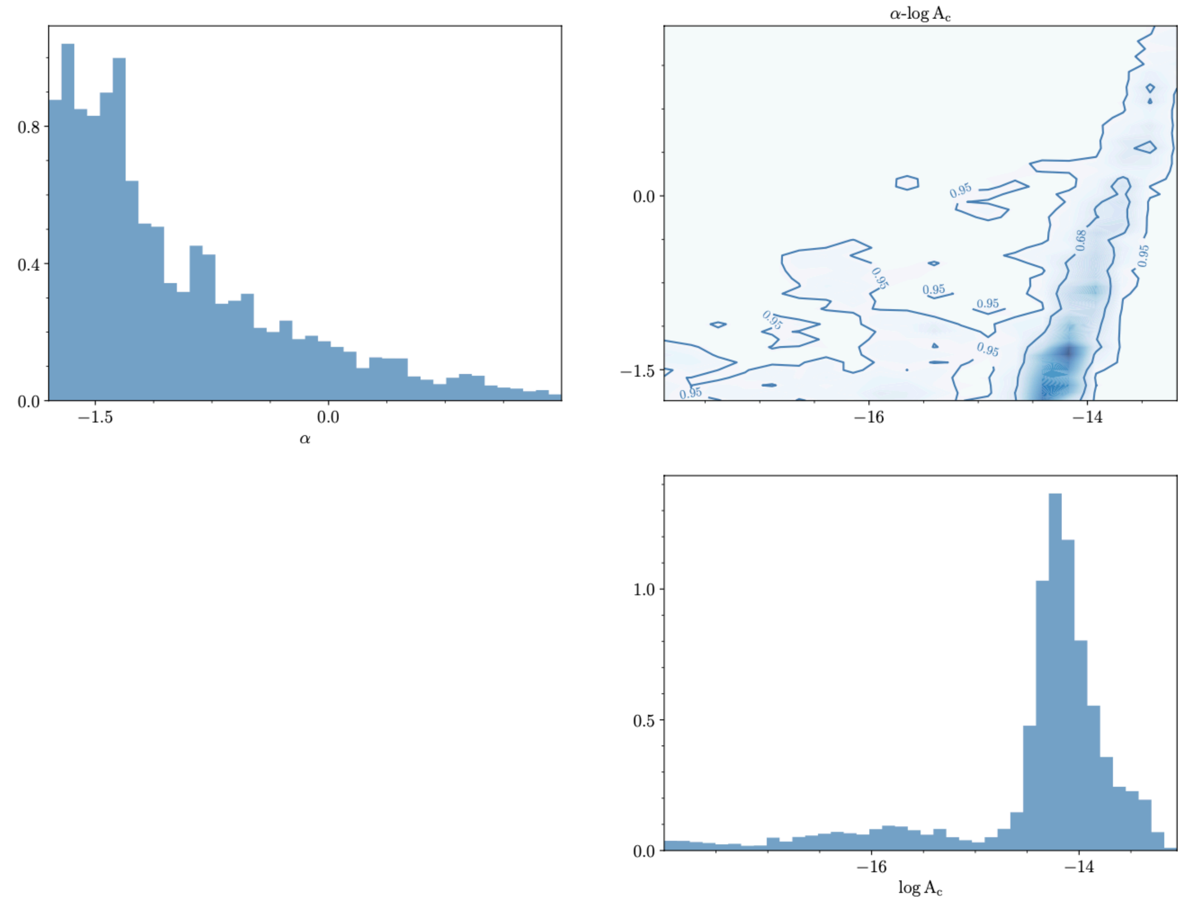

NANOGrav collaboration, ApJL 951:L8 (arXiv:2306.16213)
Antoniadis et al., A&A (arXiv:2306.16214)
Reardon et al., ApJL (arXiv:2306.16215)
Xu et al., RAA 23:075024 (arXiv:2306.16216)

NANOGrav 15-year

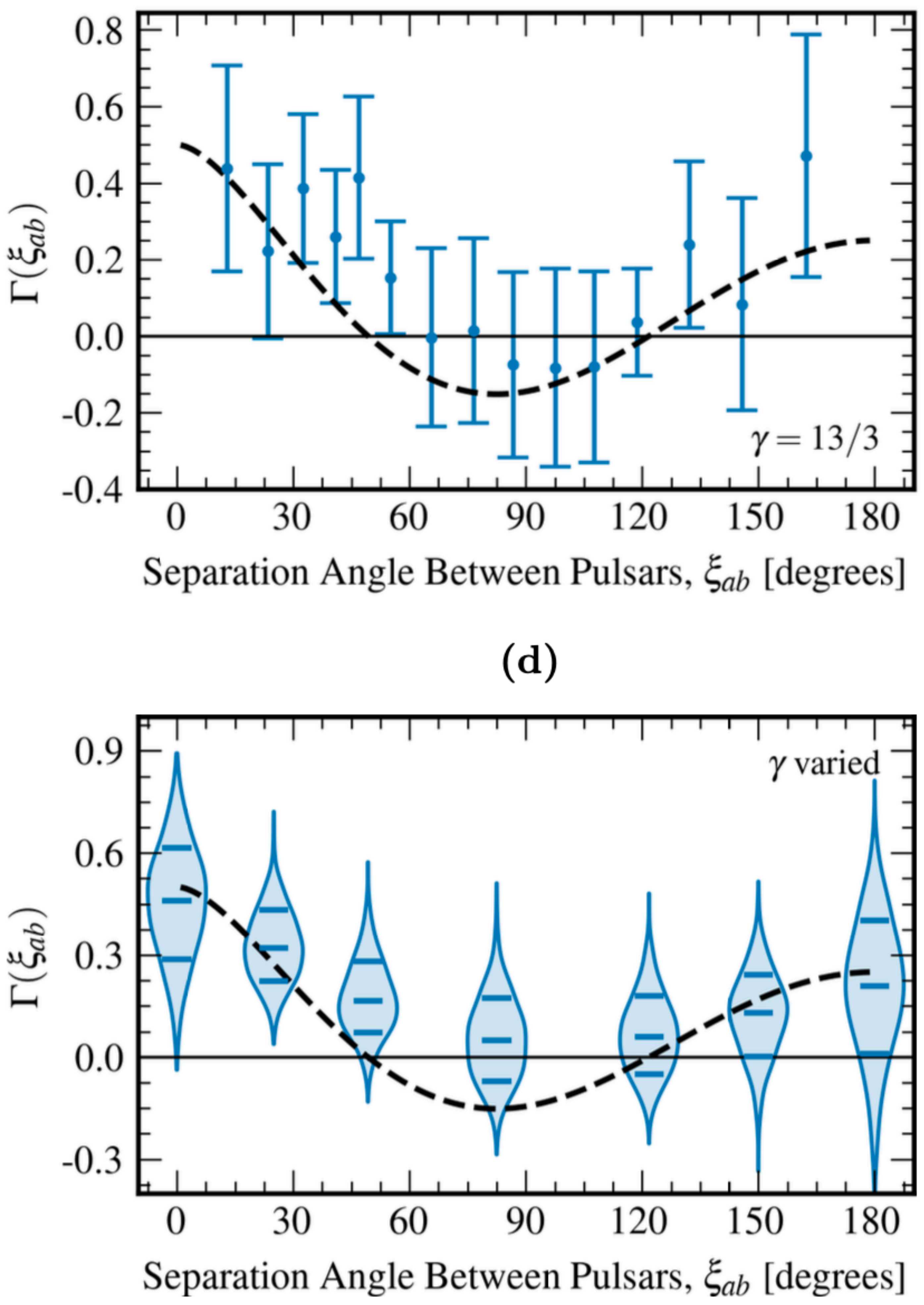

EPTA DR2

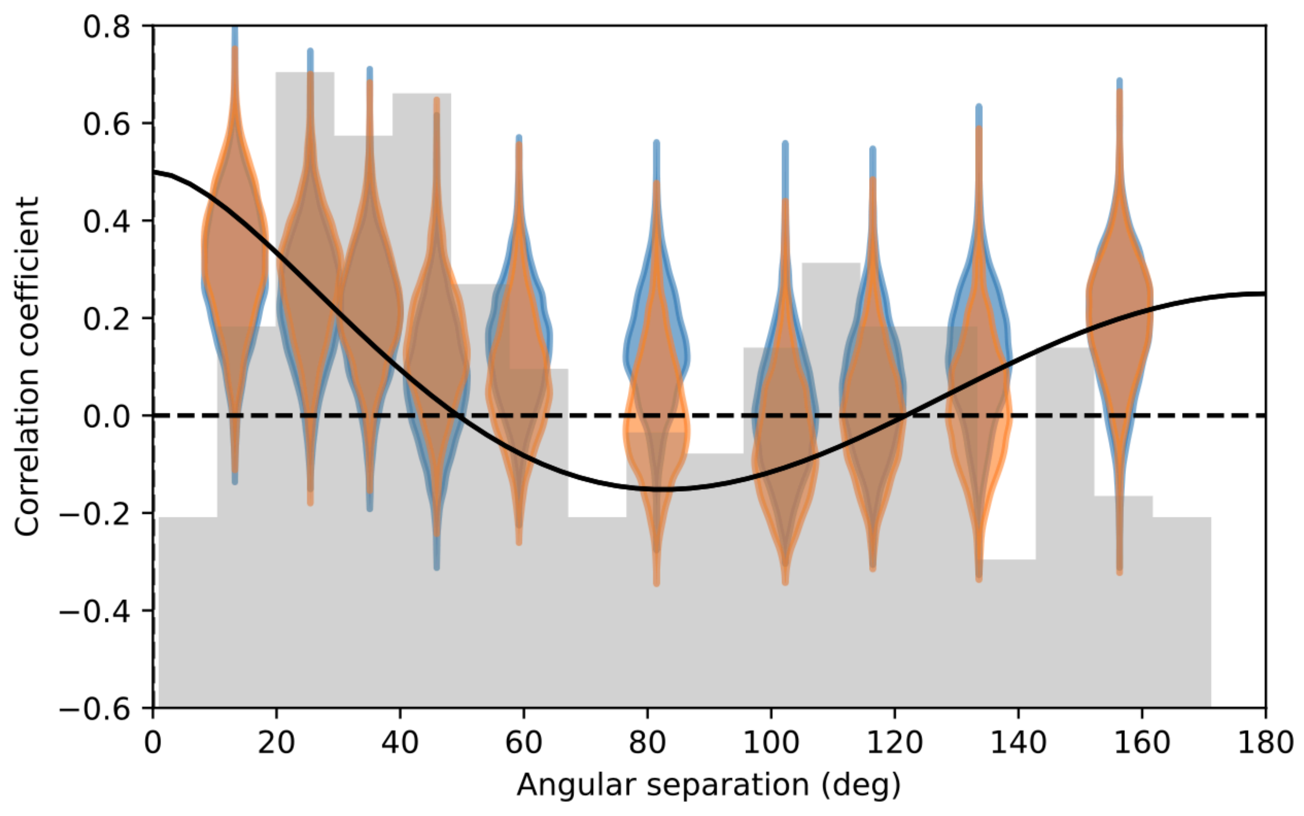

PPTA DR3

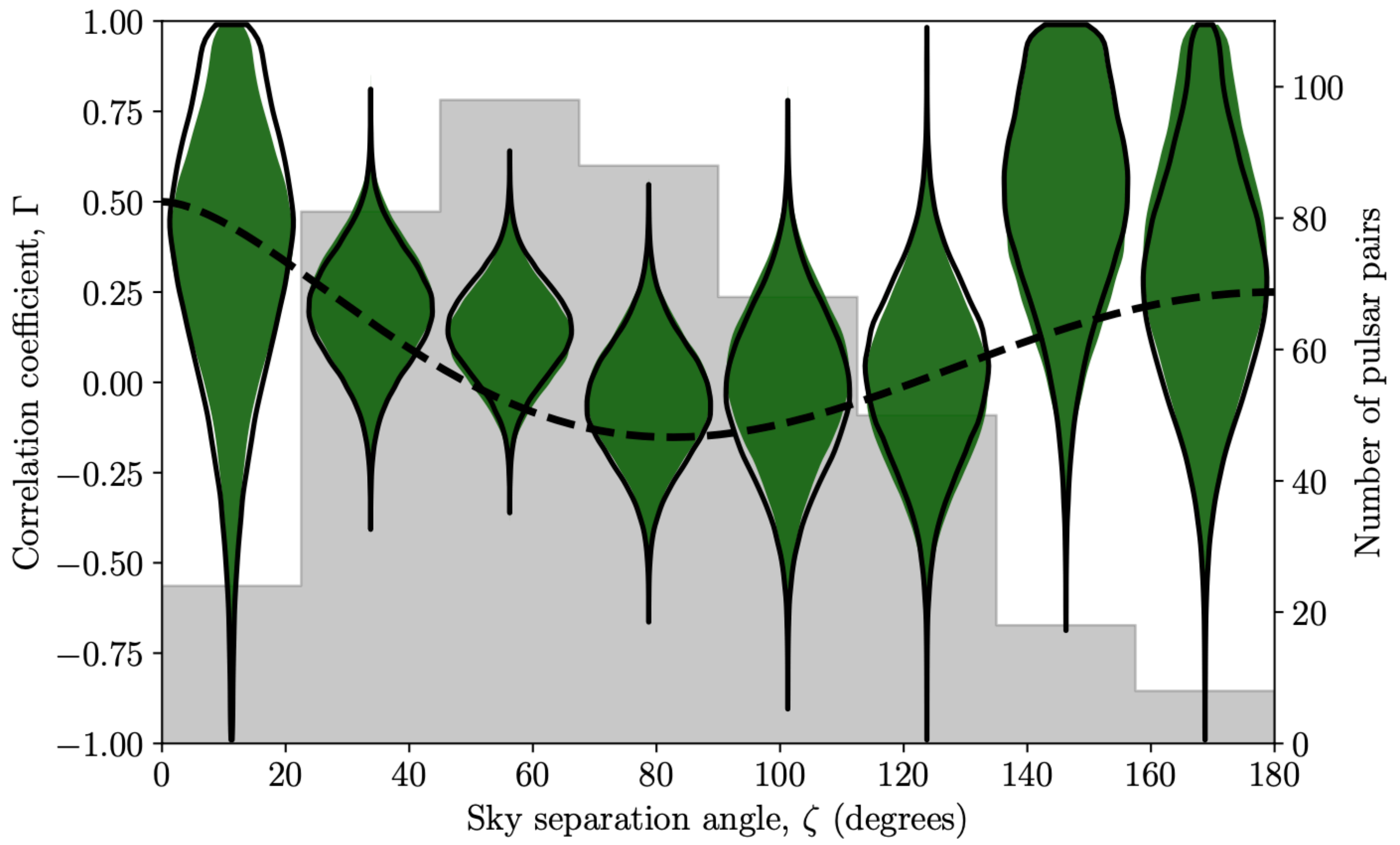

CPTA DR1

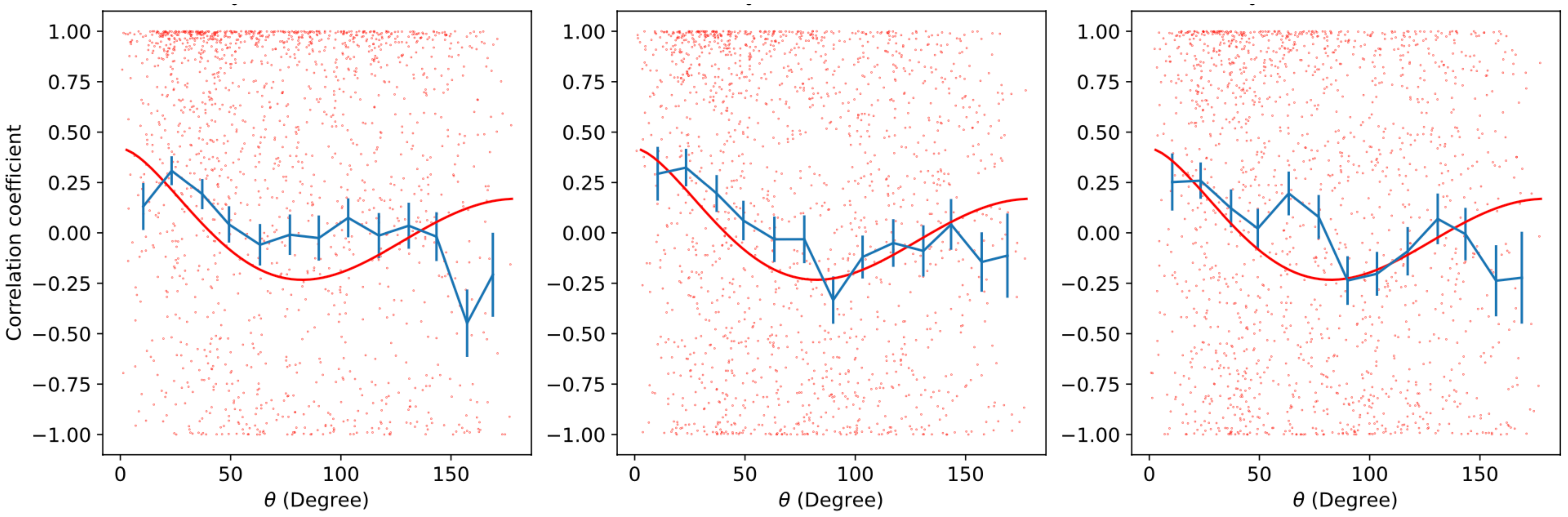

NANOGrav collaboration, ApJL 951:L8 (arXiv:2306.16213)
Antoniadis et al., A&A (arXiv:2306.16214)
Reardon et al., ApJL (arXiv:2306.16215)
Xu et al., RAA 23:075024 (arXiv:2306.16216)

NANOGrav 15-year:

We report multiple lines of evidence for a stochastic signal that is correlated among 67 pulsars from the 15-year pulsar-timing data set collected by the North American Nanohertz Observatory for Gravitational Waves. The correlations follow the Hellings–Downs pattern expected for a stochastic gravitational-wave background. The presence of such a gravitational-wave background with a power-law-spectrum is favored over a model with only independent pulsar noises with a Bayes factor in excess of 10^{14}, and this same model is favored over an uncorrelated common power-law–spectrum model with Bayes factors of 200–1000, depending on spectral modeling choices. We have built a statistical back-ground distribution for these latter Bayes factors using a method that removes inter-pulsar correlations from our data set, finding $p = 10^{-3}$ (approx. 3σ) for the observed Bayes factors in the null no-correlation scenario. A frequentist test statistic built directly as a weighted sum of inter-pulsar correlations yields $p = 5 \times 10^{-5} - 1.9 \times 10^{-4}$ (approx. $3.5 - 4\sigma$). Assuming a fiducial $f^{-2/3}$ characteristic-strain spectrum, as appropriate for an ensemble of binary supermassive black-hole inspirals, the strain amplitude is $2.4^{+0.7}_{-0.6} \times 10^{-15}$ (median +90% credible interval) at a reference frequency of 1 yr^{-1}. The inferred gravitational-wave background amplitude and spectrum are consistent with astrophysical expectations for a signal from a population of supermassive black-hole binaries, although more exotic cosmological and astrophysical sources cannot be excluded. The observation of Hellings–Downs correlations points to the gravitational-wave origin of this signal.

NANOGrav collaboration, ApJL 951:L8 (arXiv:2306.16213)

EPTA DR2:

We present the results of the search for an isotropic stochastic gravitational wave background (GWB) at nanohertz frequencies using the second data release of the European Pulsar Timing Array (EPTA) for 25 millisecond pulsars and a combination with the first data release of the Indian Pulsar Timing Array (InPTA). A robust GWB detection is conditioned upon resolving the Hellings-Downs angular pattern in the pairwise cross-correlation of the pulsar timing residuals. Additionally, the GWB is expected to yield the same (common) spectrum of temporal correlations across pulsars, which is used as a null hypothesis in the GWB search. Such a common-spectrum process has already been observed in pulsar timing data. We analysed (i) the full 24.7-year EPTA data set, (ii) its 10.3-year subset based on modern observing systems, (iii) the combination of the full data set with the first data release of the InPTA for ten commonly timed millisecond pulsars, and (iv) the combination of the 10.3-year subset with the InPTA data. These combinations allowed us to probe the contributions of instrumental noise and interstellar propagation effects. With the full data set, we find marginal evidence for a GWB, with a Bayes factor of four and a false alarm probability of 4%. With the 10.3-year subset, we report evidence for a GWB, with a Bayes factor of 60 and a false alarm probability of about 0.1% ($\gtrsim 3\sigma$ significance). The addition of the InPTA data yields results that are broadly consistent with the EPTA-only data sets, with the benefit of better noise modelling. Analyses were performed with different data processing pipelines to test the consistency of the results from independent software packages. The latest EPTA data from new generation observing systems show non-negligible evidence for the GWB. At the same time, the inferred spectrum is rather uncertain and in mild tension with the common signal measured in the full data set. However, if the spectral index is fixed at 13/3, the two data sets give a similar amplitude of $(2.5 \pm 0.7) \times 10^{-15}$ at a reference frequency of 1 yr^{-1} . Further investigation of these issues is required for reliable astrophysical interpretations of this signal. By continuing our detection efforts as part of the International Pulsar Timing Array (IPTA), we expect to be able to improve the measurement of spatial correlations and better characterise this signal in the coming years..

Antoniadis et al., A&A (arXiv:2306.16214)

PPTA DR3:

Pulsar timing arrays aim to detect nanohertz-frequency gravitational waves (GWs). A background of GWs modulates pulsar arrival times and manifests as a stochastic process, common to all pulsars, with a signature spatial correlation. Here we describe a search for an isotropic stochastic gravitational-wave background (GWB) using observations of 30 millisecond pulsars from the third data release of the Parkes Pulsar Timing Array (PPTA), which spans 18 years. Using current Bayesian inference techniques we recover and characterize a common-spectrum noise process. Represented as a strain spectrum $h_c = A(f/1yr^{-1})^{\alpha}$, we measure $A = 3.1^{+1.3}_{-0.9} \times 10^{-15}$ and $\alpha = -0.45 \pm 0.20$ respectively (median and 68% credible interval). For a spectral index of $\alpha = -2/3$, corresponding to an isotropic background of GWs radiated by inspiraling supermassive black hole binaries, we recover an amplitude of $A = 2.04^{+0.25}_{-0.22} \times 10^{-15}$. However, we demonstrate that the apparent signal strength is time-dependent, as the first half of our data set can be used to place an upper limit on A that is in tension with the inferred common-spectrum amplitude using the complete data set. We search for spatial correlations in the observations by hierarchically analyzing individual pulsar pairs, which also allows for significance validation through randomizing pulsar positions on the sky. For a process with $\alpha = -2/3$, we measure spatial correlations consistent with a GWB, with an estimated false-alarm probability of $p \lesssim 0.02$ (approx. 2σ). The long timing baselines of the PPTA and the access to southern pulsars will continue to play an important role in the International Pulsar Timing Array.

Reardon et al., ApJL (arXiv:2306.16215)

CPTA DR1:

Observing and timing a group of millisecond pulsars with high rotational stability enables the direct detection of gravitational waves (GWs). The GW signals can be identified from the spatial correlations encoded in the times-of-arrival of widely spaced pulsar-pairs. The Chinese Pulsar Timing Array (CPTA) is a collaboration aiming at the direct GW detection with observations carried out using Chinese radio telescopes. This short article serves as a "table of contents" for a forthcoming series of papers related to the CPTA Data Release 1 (CPTA DR1) which uses observations from the Five-hundred-meter Aperture Spherical radio Telescope (FAST). Here, after summarizing the time span and accuracy of CPTA DR1, we report the key results of our statistical inference finding a correlated signal with amplitude $logA_c = -14.4^{+1.0}_{-2.8}$ for spectral index in the range of $\alpha \in [-1.8, 1.5]$ assuming a GW background (GWB) induced quadrupolar correlation. The search for the Hellings–Downs (HD) correlation curve is also presented, where some evidence for the HD correlation has been found that a $4.6 - \sigma$ statistical significance is achieved using the discrete frequency method around the frequency of 14 nHz. We expect that the future International Pulsar Timing Array data analysis and the next CPTA data release will be more sensitive to the nHz GWB, which could verify the current results.

Xu et al., RAA 23:075024 (arXiv:2306.16216)

Estimated sensitivity to the characteristic strain

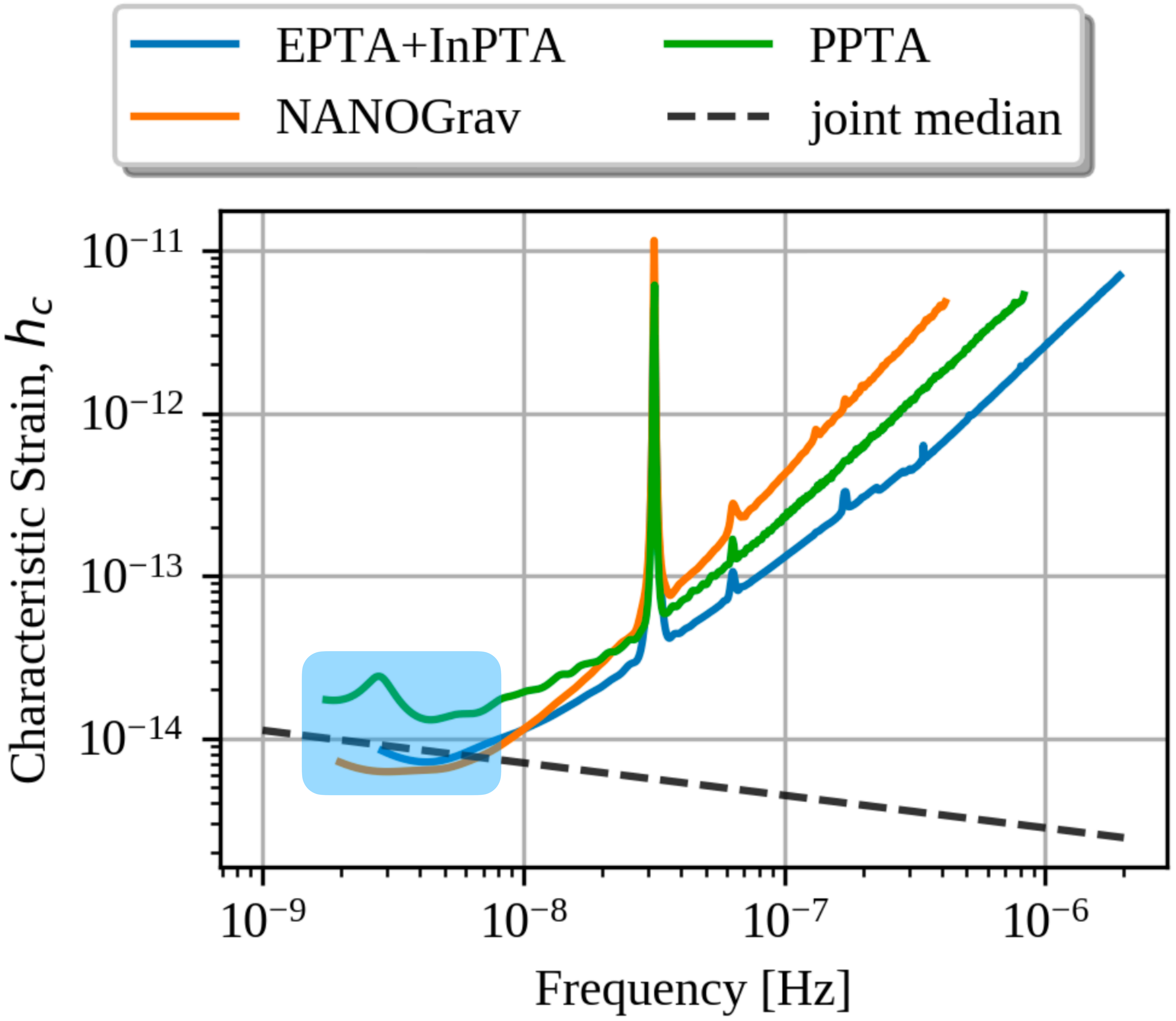

IPTA collaboration, arXiv:2309.00693

SuperMassive Black Hole Binaries

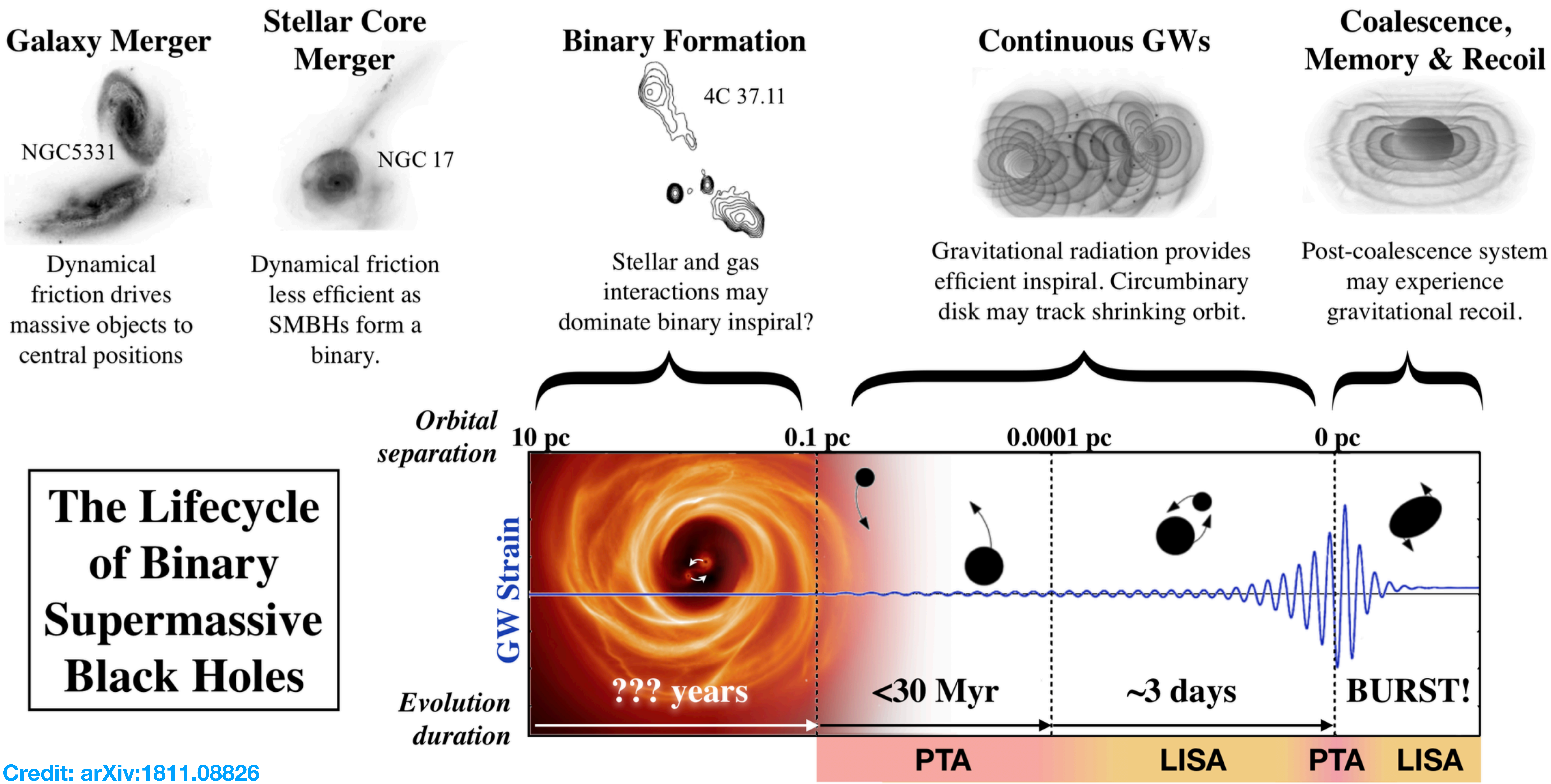

Credit: arXiv:1811.08826

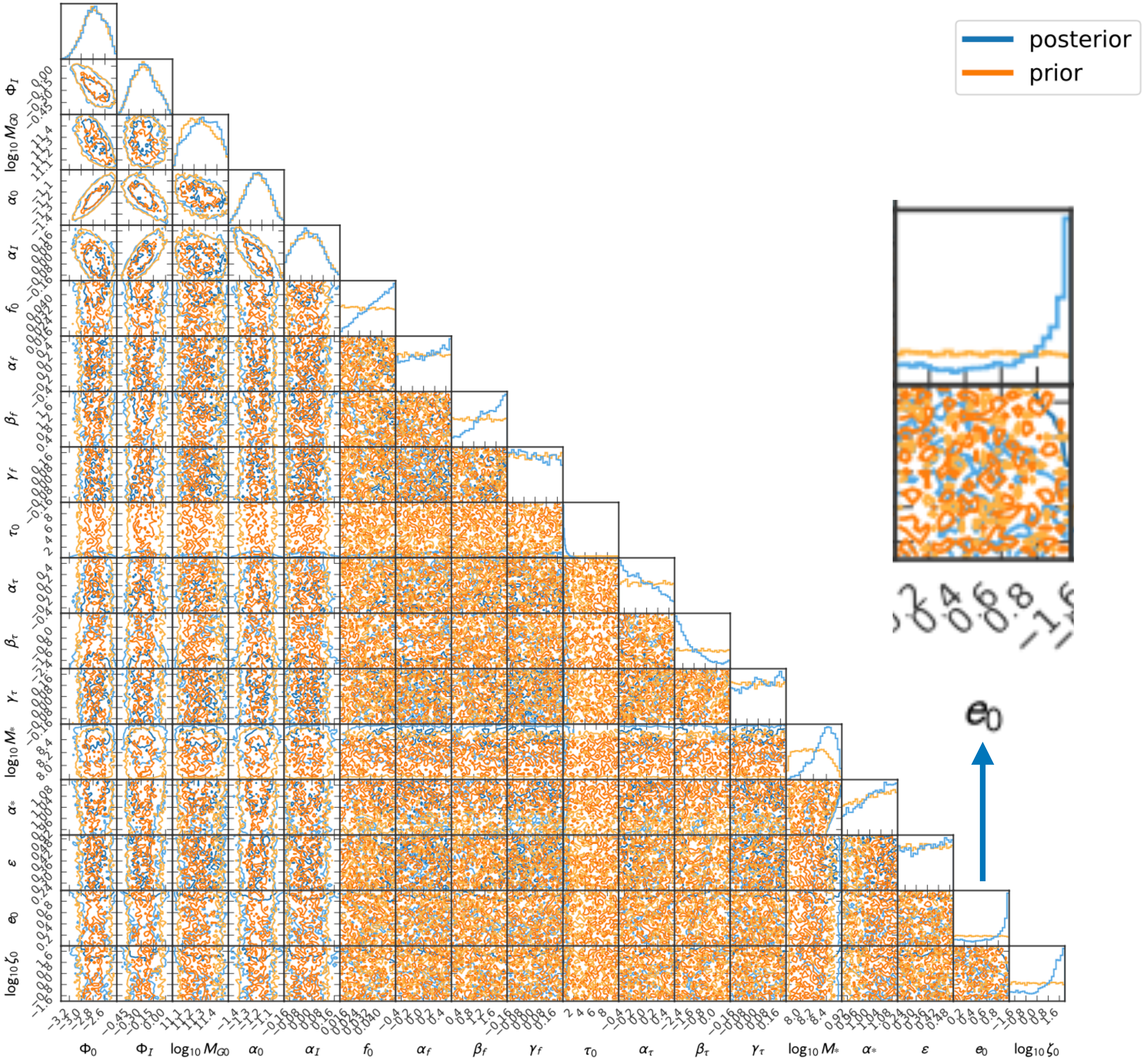

18 parameters for the astro-informed formation model [Chen, Sesana & Conselice, MNRAS (2019), arXiv:1810.04184]

Galaxy stellar mass function (GSMF)
Galaxy pair fraction
Galaxy merger timescale
Bulge-SMBH relation
Stellar and SMBHB condition

parameter	description	prior
	GSMF	
Φ_0	GSMF norm	$-2.77^{+0.27}_{-0.29}$
Φ_I	GSMF norm redshift evolution	$-0.27^{+0.23}_{-0.21}$
$\log_{10} M_{G0}$	GSMF scaling mass	$11.24^{+0.20}_{-0.17}$
α_0	GSMF mass slope	$-1.24^{+0.16}_{-0.16}$
α_I	GSMF mass slope redshift evolution	$-0.03^{+0.16}_{-0.14}$
	Galaxy pair function	
f_0	pair fraction norm	Uniform $[0.01, 0.05]$
α_f	pair fraction mass slope	Uniform $[-0.5, 0.5]$
β_f	pair fraction redshift slope	Uniform $[0, 2]$
γ_f	pair fraction mass ratio slope	Uniform $[-0.2, 0.2]$
	Galaxy merger timescale	
τ_0	merger time norm	Uniform $[0.1, 10]$
α_τ	merger time mass slope	Uniform $[-0.5, 0.5]$
β_τ	merger time redshift slope	Uniform $[-3, 1]$
γ_τ	merger time mass ratio slope	Uniform $[-0.2, 0.2]$
	$M_{\rm bulge}$-$M_{\rm BH}$ relation	
$\log_{10} M_*$	$M_{\rm bulge}$-$M_{\rm BH}$ relation norm	$8.17^{+0.35}_{-0.32}$
α_*	$M_{\rm bulge}$-$M_{\rm BH}$ relation slope	$1.01^{+0.08}_{-0.10}$
ϵ	$M_{\rm bulge}$-$M_{\rm BH}$ relation scatter	Uniform $[0.2, 0.5]$
	Stellar and SMBHB condition	
e_0	SMBHB initial eccentricity	Uniform $[0.01, 0.99]$
$\log_{10} \zeta_0$	stellar density factor	Uniform $[-2, 2]$

Bi, Wu, Chen & QGH, SCPMA 66(2023)120402

Gravitational-Wave Background from SMBHBs

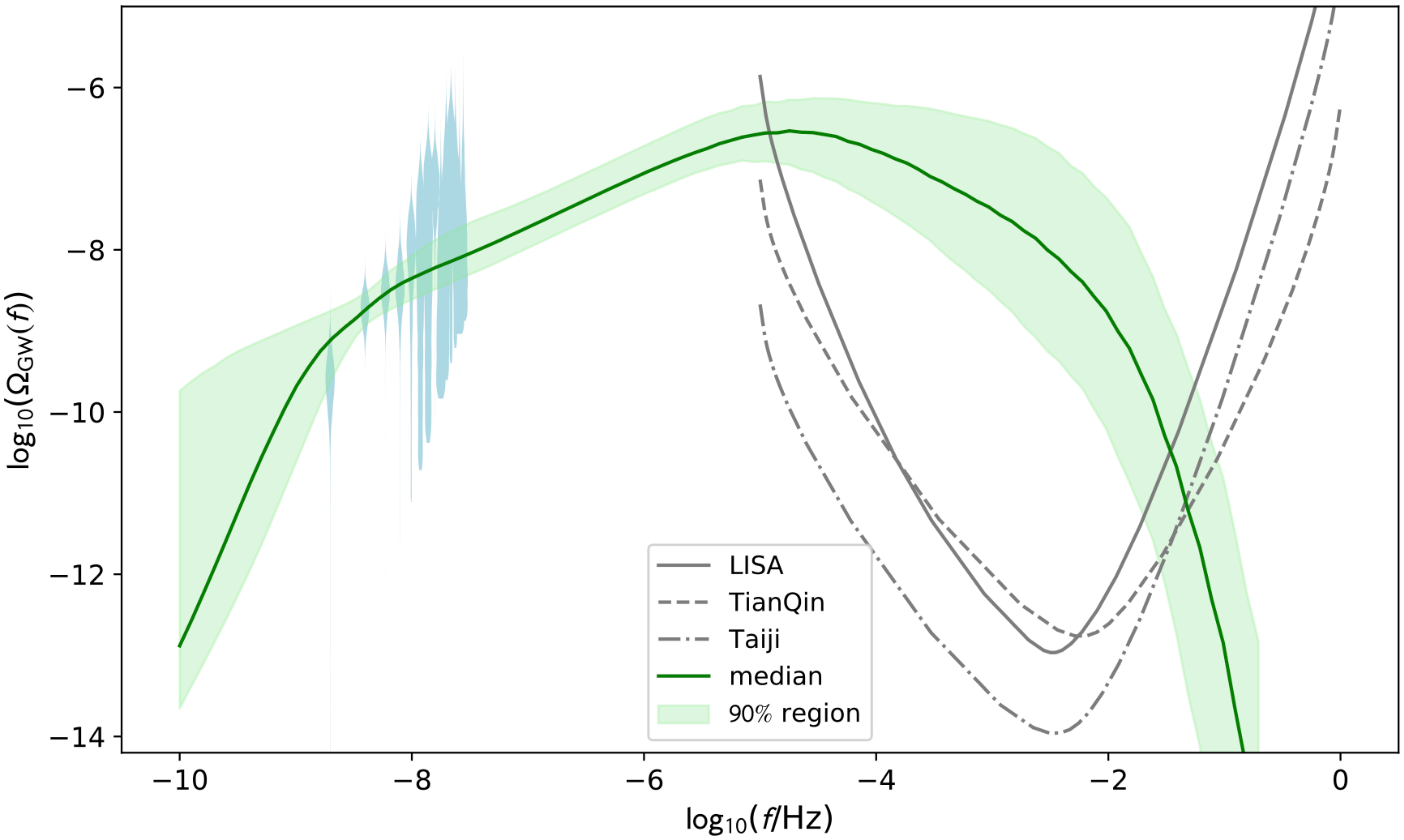

Bi, Wu, Chen & QGH, SCPMA 66(2023)120402

Conclusion and Discussion

- Recently NANOGrav, EPTA, PPTA and CPTA independently reported strong evidence for a stochastic signal consistent with Gravitational-Wave Background (GWB). Although we do not have substantial evidence yet, we may be beginning to detect a GWB.
- Supermassive Black Hole Binaries (SMBHBs) provide one of the most promising GW sources for the stochastic signal detected by PTAs.
- In addition to SMBHBs, more exotic cosmological sources can also produce detectable GWBs in the nHz range. [NANOGrav collaboration, Astrophys.J.Lett. (2023), Antoniadis et al., arXiv:2306.16227]

- Einstein’s general relativity or beyond?

    1) The velocity of gravitational wave: $v_{gw} = c$ (massless)

    2) Quadrupole radiation

    3) Two tensor polarization modes

Massive graviton

$$k^\mu = (\omega, \mathbf{k}) : \ \ \omega = \sqrt{m_g^2 + |\mathbf{k}|^2} \ \rightarrow \ f_{cut} = m_g \ (< 1/T \simeq 8.2 \times 10^{-24} \ eV)$$

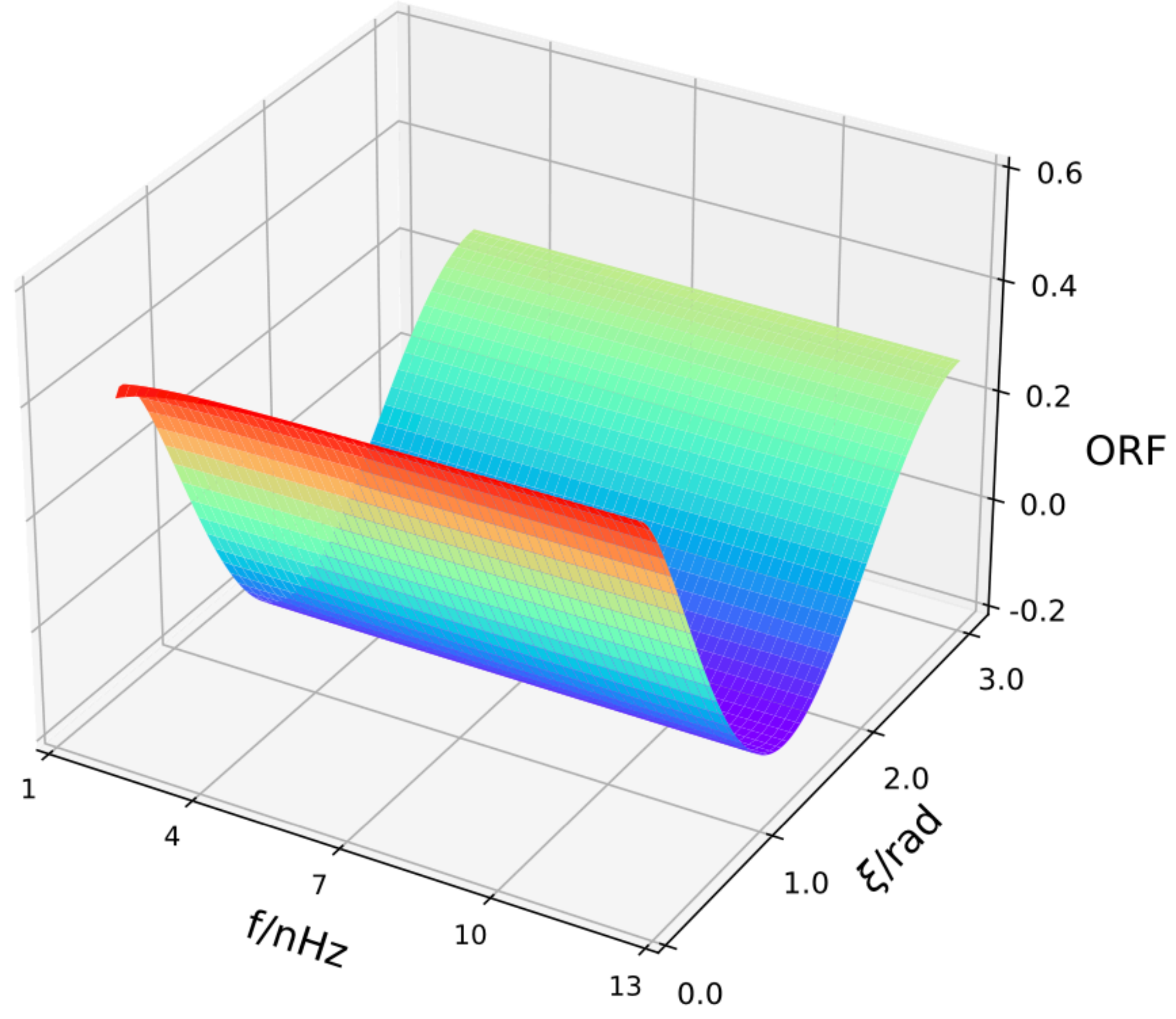

$m_g = 10^{-24}$eV

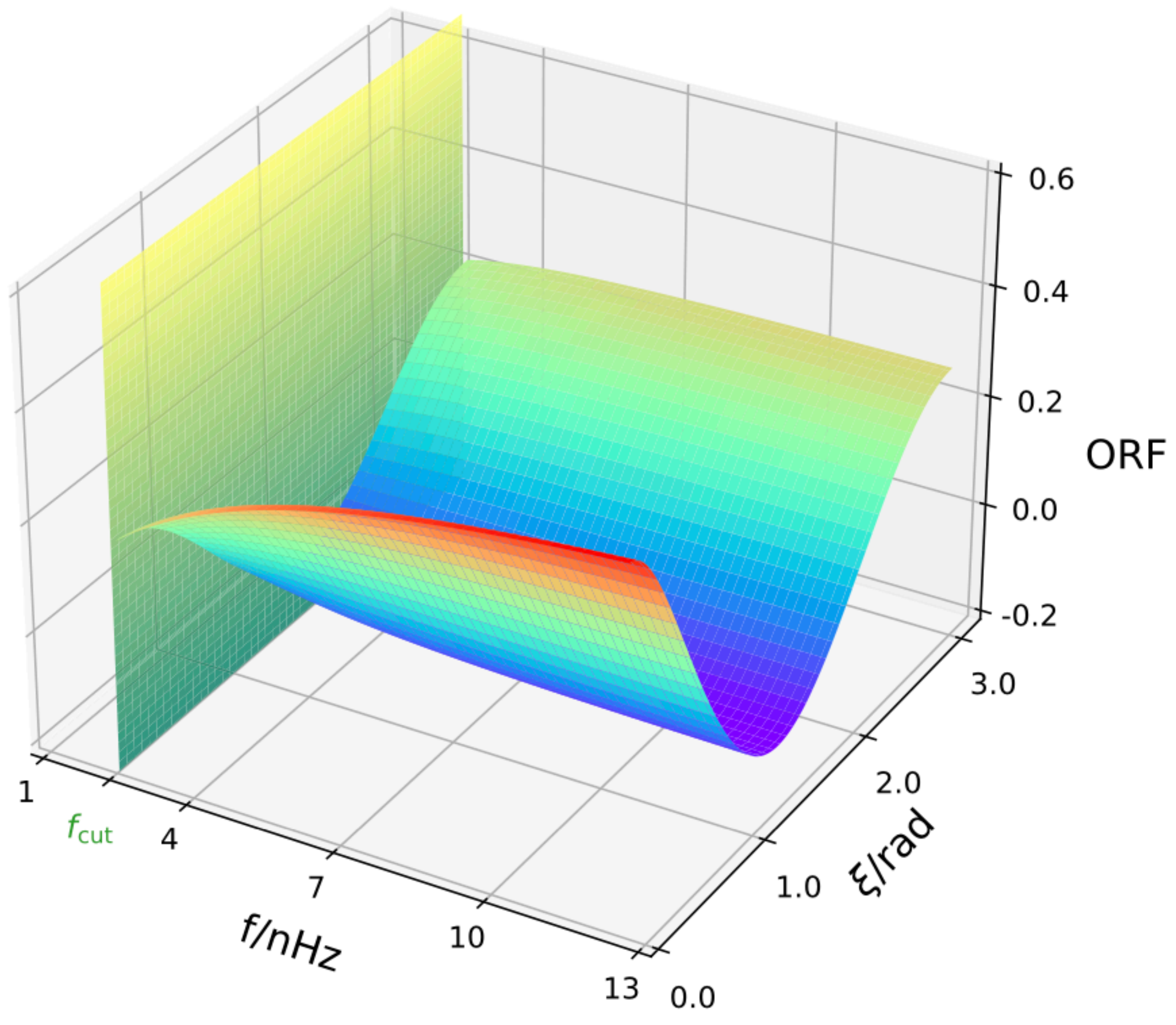

$m_g = 10^{-23}$eV

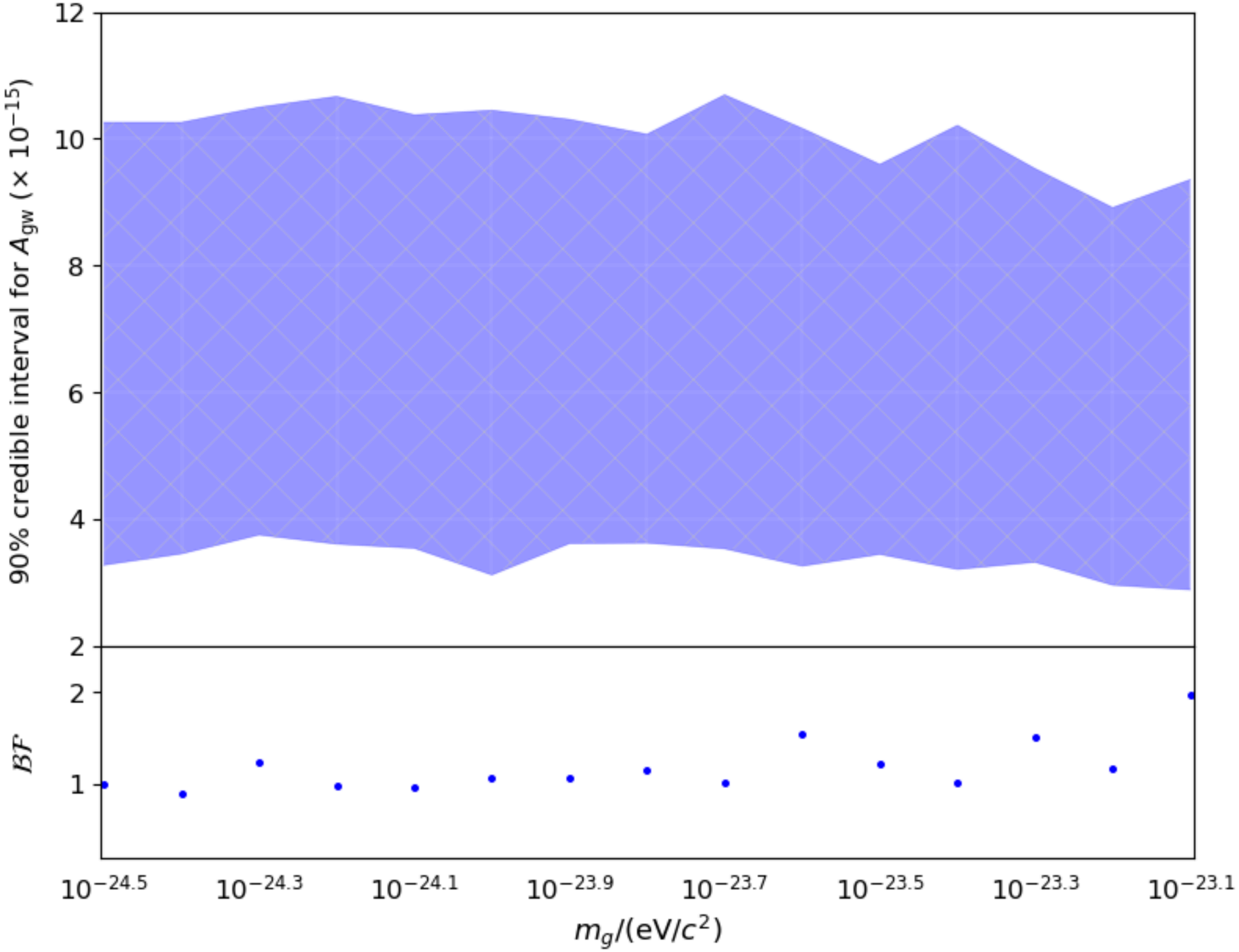

Lee et al., ApJ (2010)
Liang & Trodden, PRD (2021)
Wu, Chen & QGH, PRD (2023)

Wu, Chen, Bi & QGH, arXiv:2310.07469

Dispersion relation: $\omega = vk$

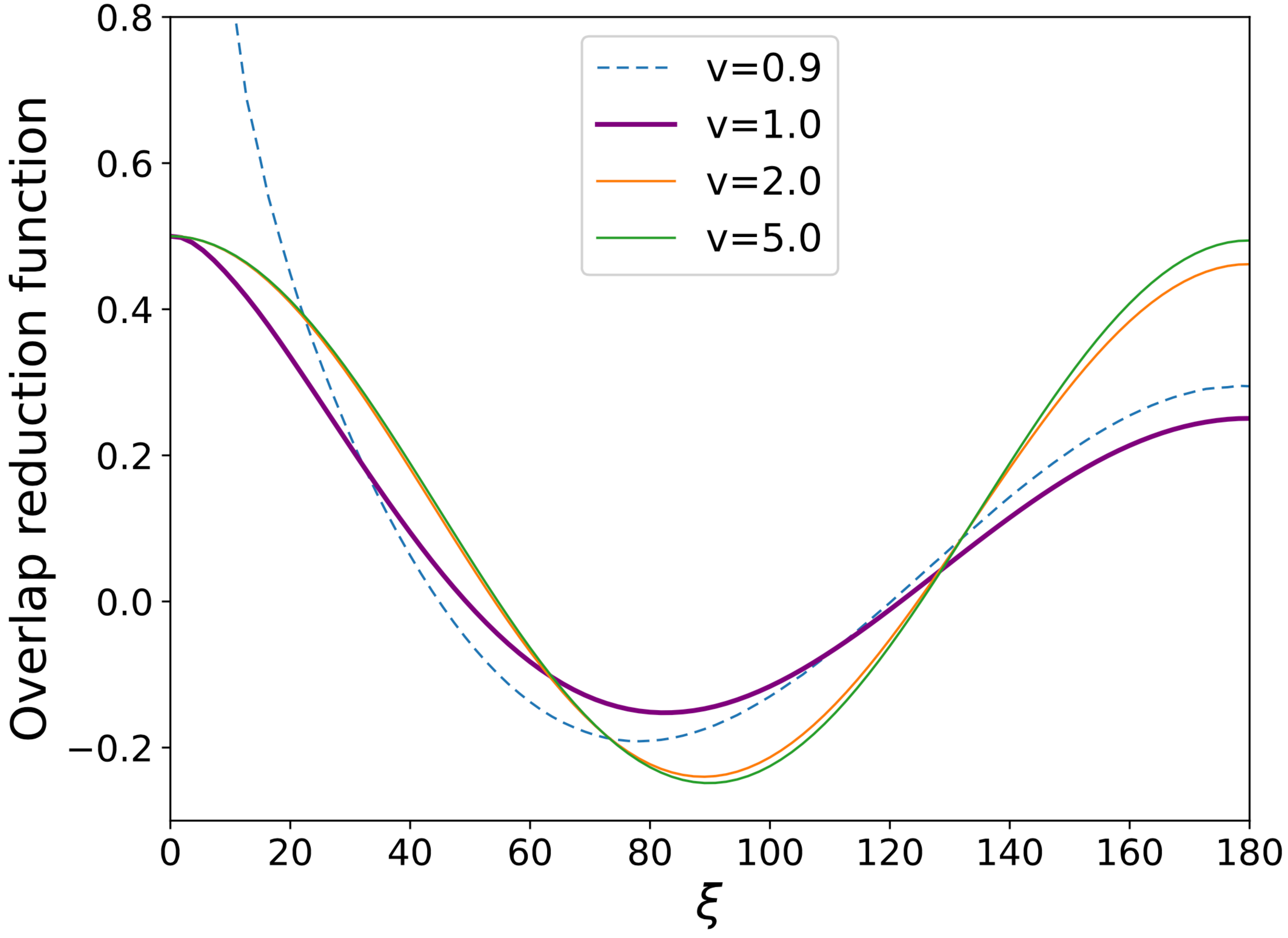

Liang, Lin & Trodden, arXiv:2304.02640

$v/c > 0.87$

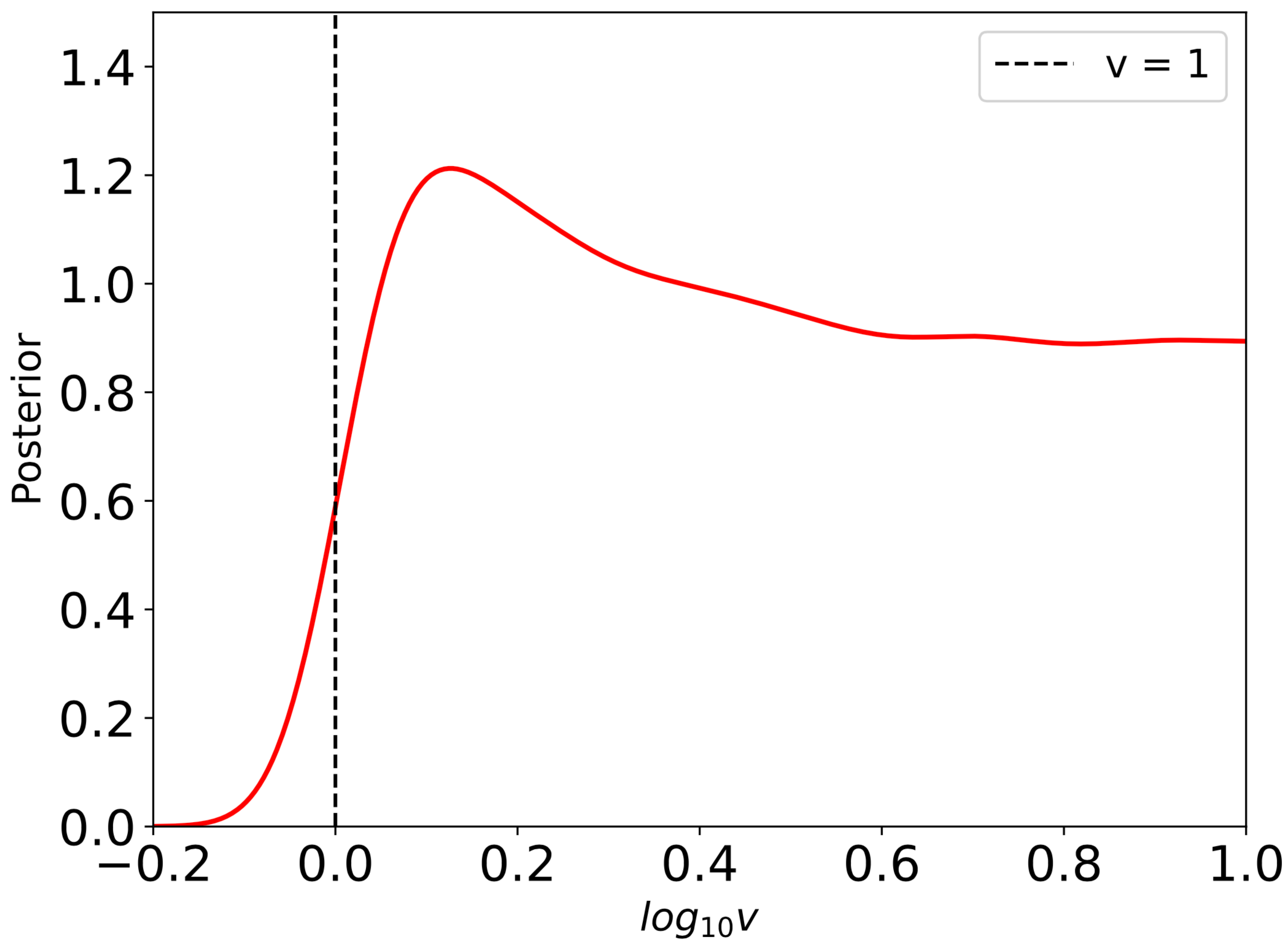

Bi, Wu, Chen & QGH, arXiv:2310. 08366

Gravitational–Wave Polarization

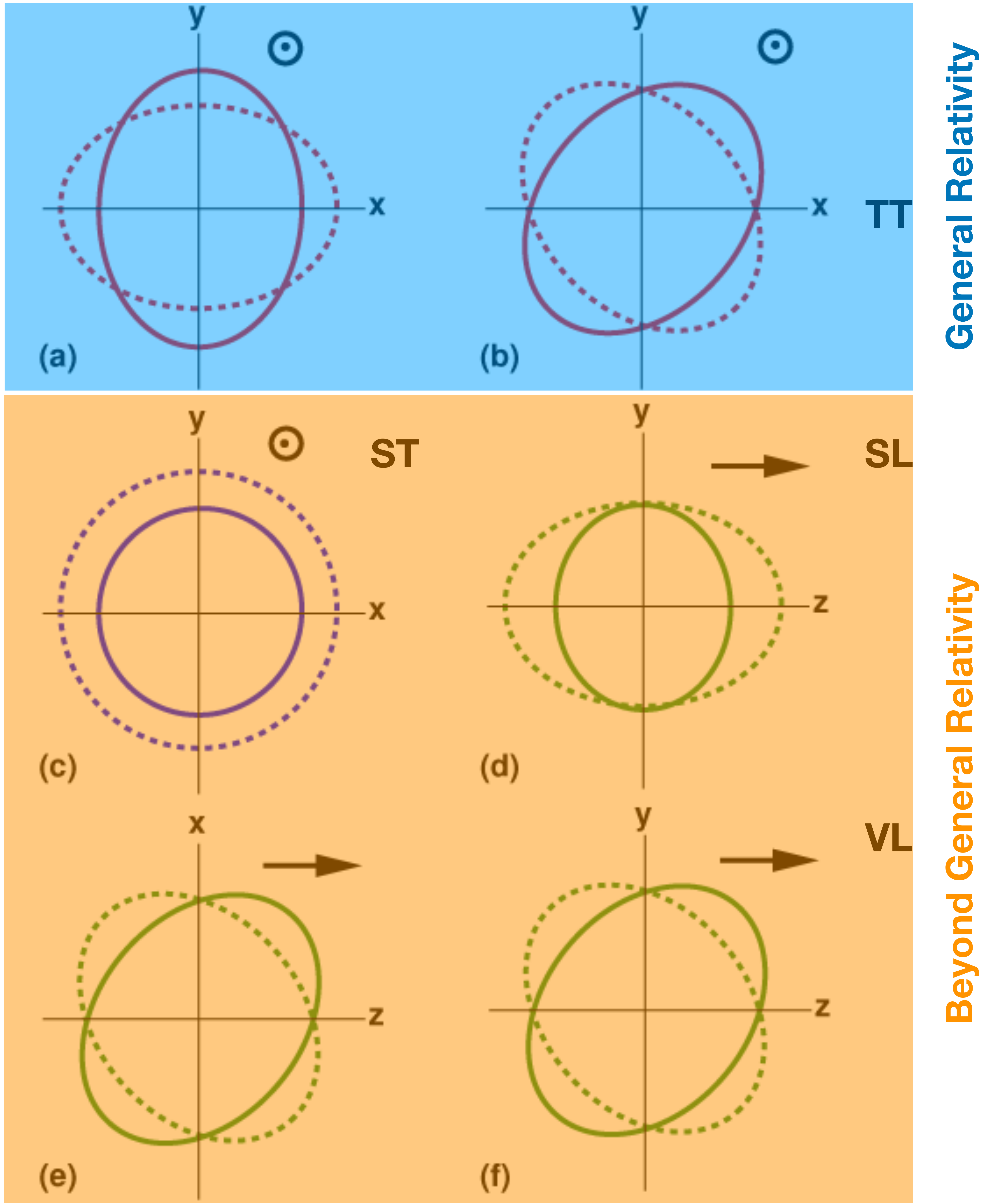

General relativity predicts that gravitational waves have two independent tensor polarization modes.

A most general metric gravity theory can allow two vector modes (VL) and two scalar modes (ST and SL) besides the two tensor modes in general relativity.

The over-lap reduced function (ORF) for TT and ST modes are given by

$$\Gamma^{TT}_{ab}(f) = \frac{1}{2}(1+\delta_{ab}) + \frac{3}{2}k_{ab}\left(\ln k_{ab} - \frac{1}{6}\right) \qquad k_{ab} = (1-\cos\xi_{ab})/2$$

$$\Gamma^{ST}_{ab}(f) = \frac{1}{8}(3+4\delta_{ab}+\cos\xi_{ab})$$

The ORF for the general transverse mode is defined by

$$\Gamma^{GT}_{ab}(f) = \frac{1}{8}(3+4\delta_{ab}+\cos\xi_{ab}) + \frac{\alpha}{2}k_{ab}\ln k_{ab}$$

which reduced to TT for $\alpha = 3$ and ST for $\alpha = 0$.

Closed-form expressions for the SL and VL modes are not available, and have to be computed numerically.

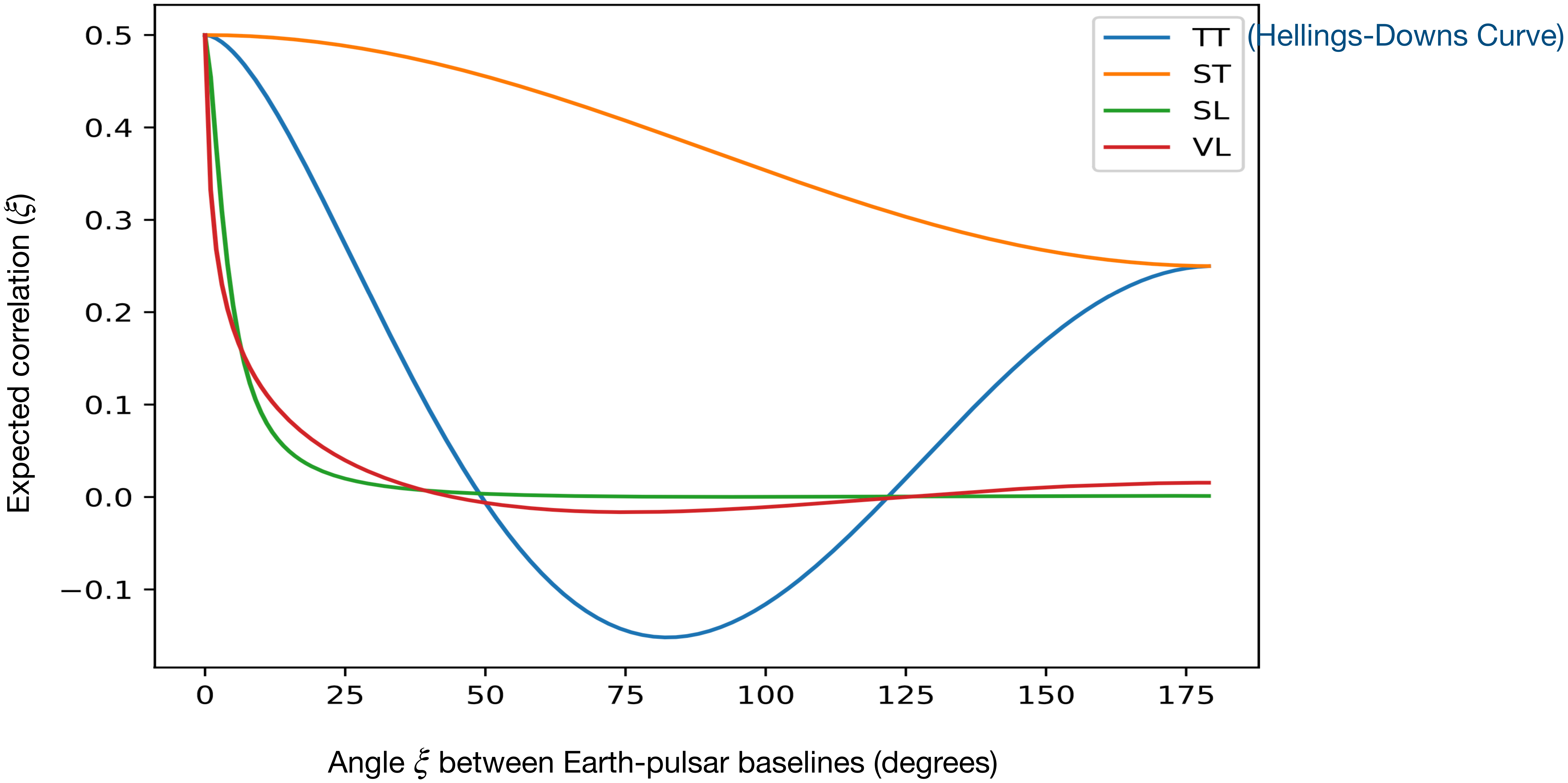

TT (Hellings-Downs Curve)
ST
SL
VL
Expected correlation (ξ)
0.5
0.4
0.3
0.2
0.1
0.0
−0.1
0
25
50
75
100
125
150
175
Angle ξ between Earth-pulsar baselines (degrees)

NANOGrav 12.5-yr

The common-spectrum process is taken as the fiducial model M_0.

ephemeris	TT	ST	VL	SL
DE438	4.96(9)	107(7)	1.94(3)	0.373(5)
BAYESEPHEM	2.35(3)	18.4(7)	1.31(2)	0.555(7)

TABLE II. The Bayes factors for various models compared to the UCP model. The digit in the parentheses gives the uncertainty on the last quoted digit.

Strong Bayesian Evidence

Lee & Wagenmakers, 2015

Bayes Factor	Interpretation
> 100	Extreme evidence for alternative hypothesis
30 – 100	Very strong evidence for alternative hypothesis
10 – 30	Strong evidence for alternative hypothesis
3 – 10	Moderate evidence for alternative hypothesis
1 – 3	Anecdotal evidence for alternative hypothesis
1	No evidence

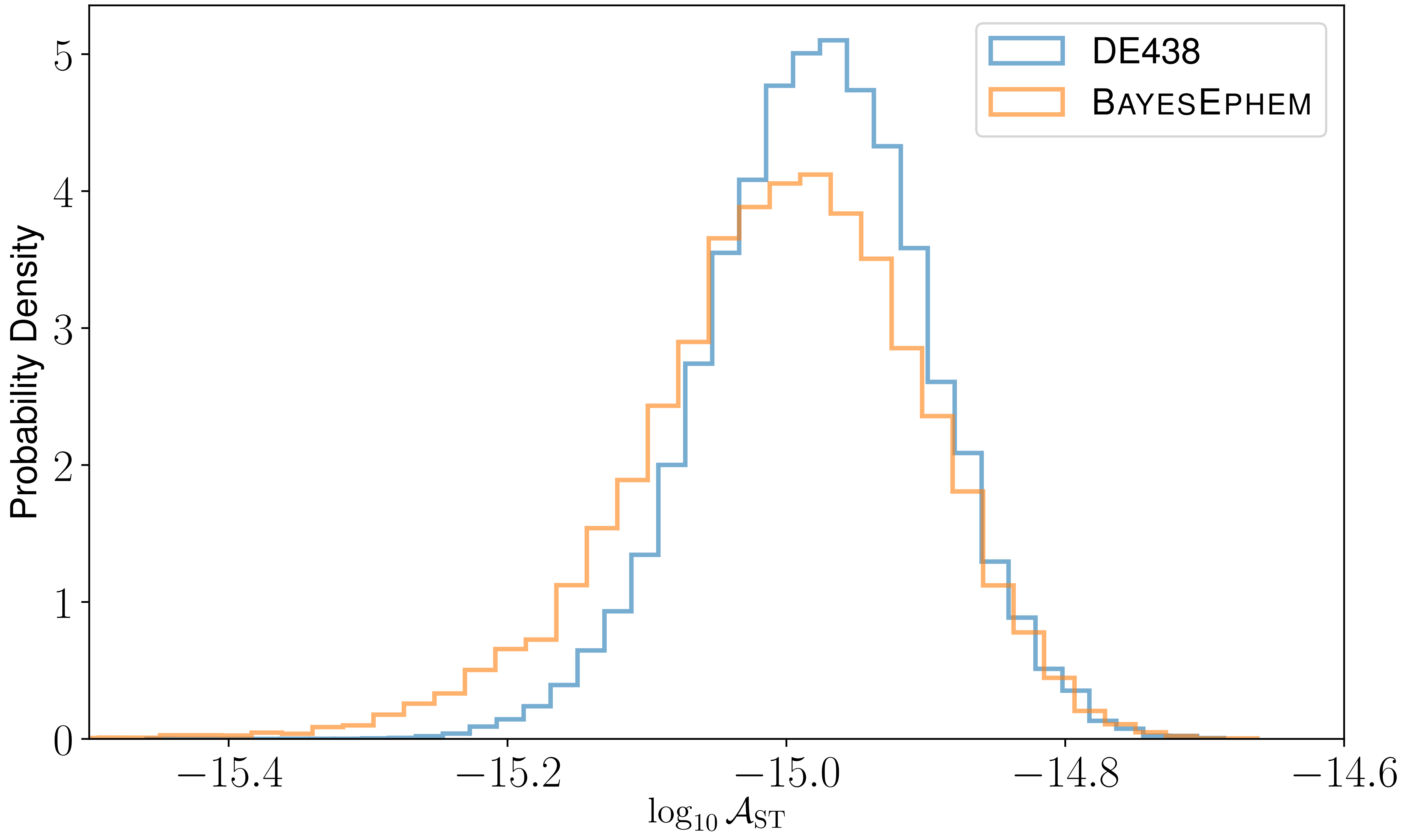

$A_{ST} = 1.06^{+0.35}_{-0.28} \times 10^{-15}$, **or**, $\Omega^{ST}_{GW} = 1.54^{+1.21}_{-0.71} \times 10^{-9}$

(90% confidence level)

Chen, Yuan & QGH, SCPMA 64(2021)12, 120412 (arXiv:2101.06869)

NANOGrav 15-yr

Bayesian Factor compared to TT polarization mode

Model	ST	VL	SL	TT + ST	GT-best
BF	0.40(3)	0.12(2)	0.002(1)	0.943(5)	3.9(3)

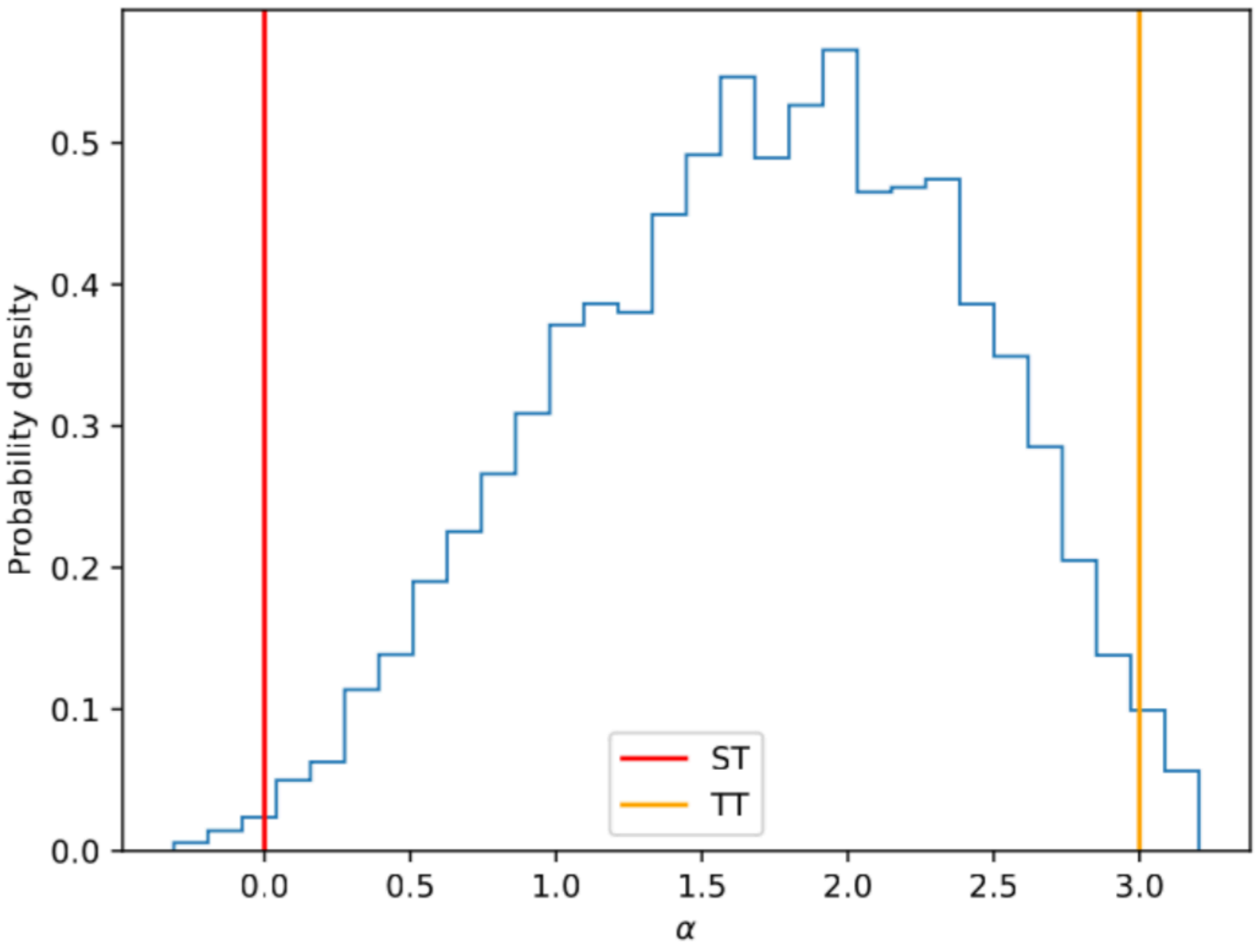

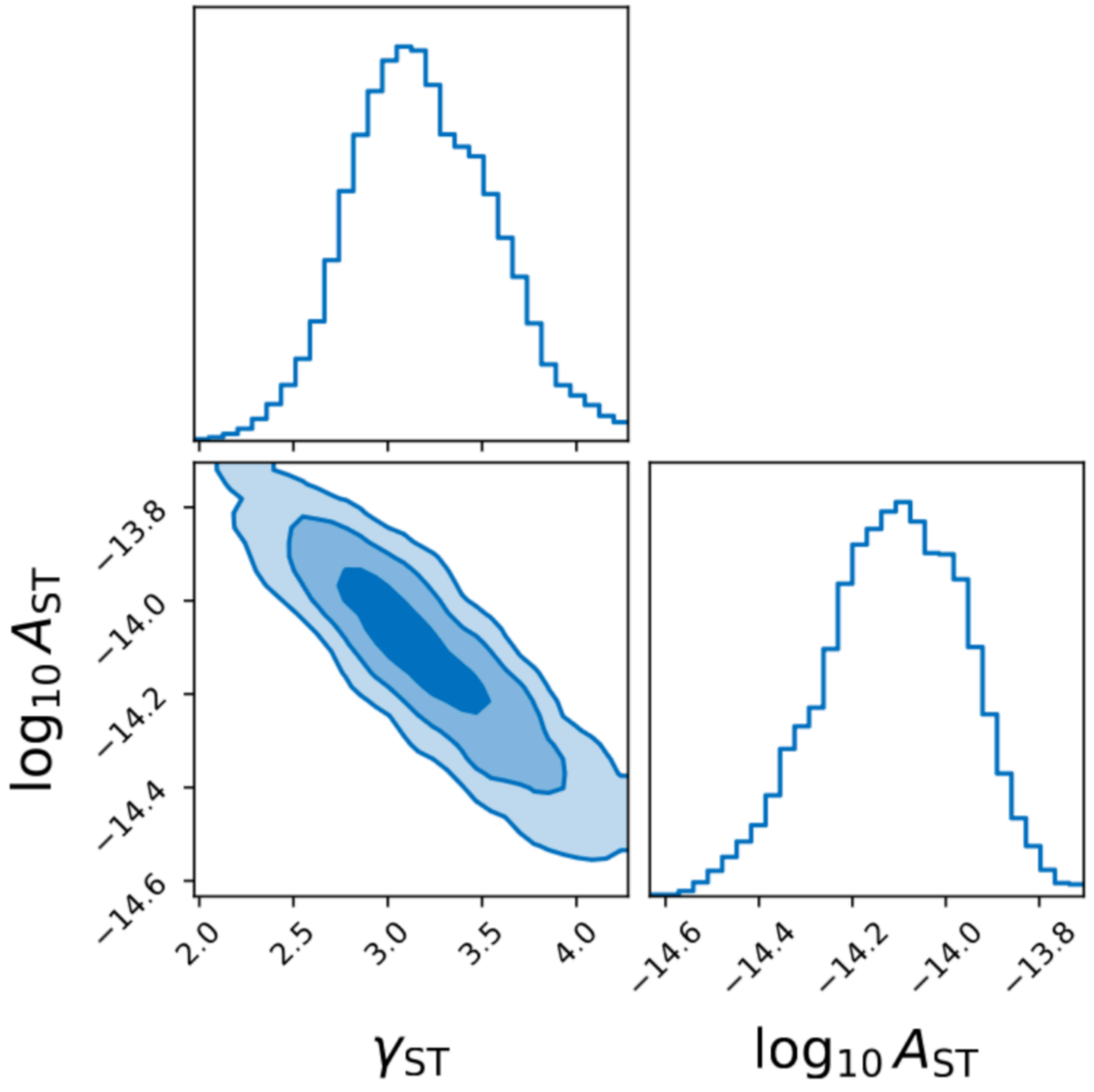

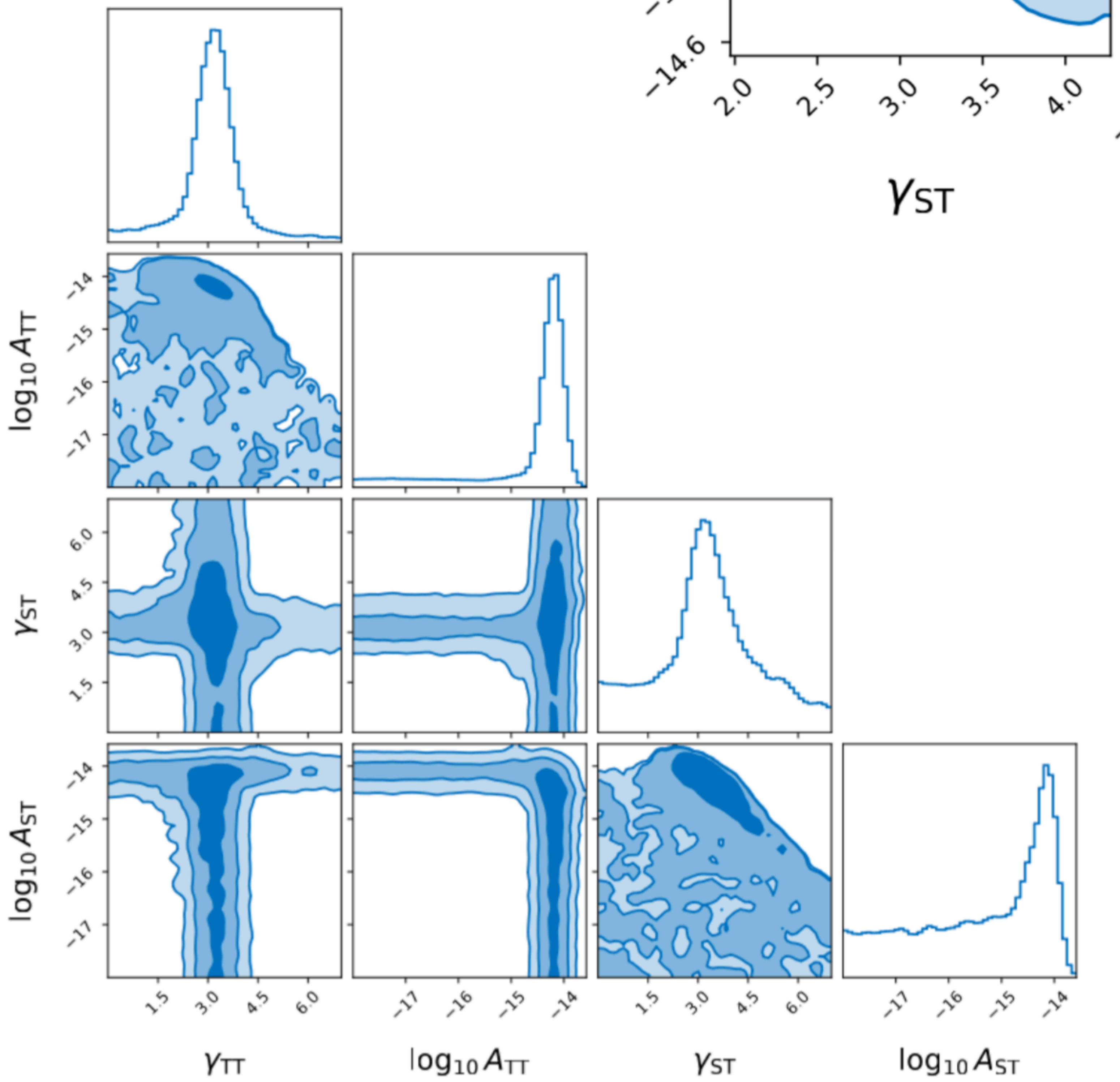

Chen, Wu, Bi & QGH, arXiv:2310.11238


Thank You!